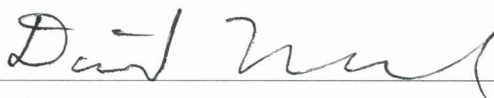


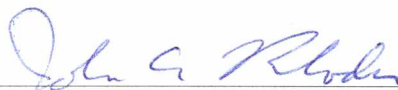
EXACT AND NUMERICAL SOLUTIONS FOR STOKES FLOW IN GLACIERS

By

William H. Mitchell

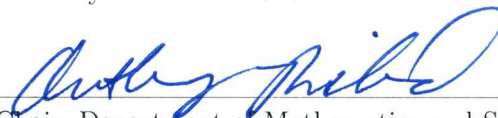
RECOMMENDED:





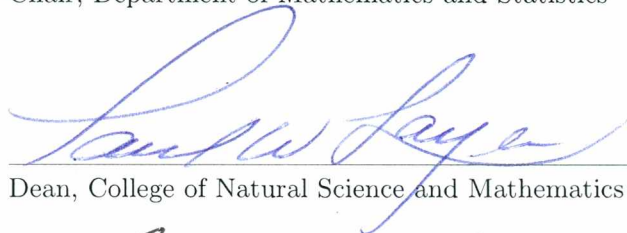


Advisory Committee Chair



Chair, Department of Mathematics and Statistics

APPROVED:



Dean, College of Natural Science and Mathematics



Dean of the Graduate School



Date

EXACT AND NUMERICAL SOLUTIONS FOR STOKES FLOW IN GLACIERS

A
THESIS

Presented to the Faculty
of the University of Alaska Fairbanks
in Partial Fulfillment of the Requirements
for the Degree of
MASTER OF SCIENCE

By
William H. Mitchell, B.A.

Fairbanks, Alaska

August 2012

Abstract

We begin with an overview of the fluid mechanics governing ice flow. We review a 1985 result due to Balise and Raymond giving exact solutions for a glaciologically-relevant Stokes problem. We extend this result by giving exact formulas for the pressure and for the basal stress. This leads to a theorem giving a necessary condition on the basal velocity of a gravity-induced flow in a rectangular geometry. We describe the finite element method for solving the same problem numerically. We present a concise implementation using FEniCS, a freely-available software package, and discuss the convergence of the numerical method to the exact solution. We describe how to fix an error in a recent published model.

Table of Contents

	Page
Signature Page	i
Title Page	ii
Abstract	iii
Table of Contents	iv
List of Figures	vi
Acknowledgments	vii
Chapter 1 Introduction	1
Chapter 2 Preliminaries	3
2.1 Introduction	3
2.2 Elementary Fluid Dynamics	4
2.2.1 Stress, pressure, and deviatoric stress	4
2.2.2 The strain rate tensor	5
2.2.3 Constitutive laws	6
2.3 The Navier-Stokes and Stokes Equations	7
2.4 The Biharmonic Equation	11
2.5 General Boundary Conditions for Glaciology	12
2.6 Boundary Conditions in the Rectangular Case	13
2.7 Sobolev Spaces	16
Chapter 3 Exact Solutions	18
3.1 The Boundary Value Problem	18
3.2 The No-Slip Case	19
3.3 The No-Gravity Case	20
3.3.1 Reduction to an ordinary differential equation	20
3.3.2 Nonzero eigenvalues	21
3.3.3 The zero eigenvalue	23
3.3.4 The nonhomogeneous boundary condition	24
3.4 Existence of Solutions for the Biharmonic Problem	25

3.5	Recovery of Velocity	26
3.6	Recovery of Pressure	27
3.7	Stress at the Lower Boundary	29
3.8	Stress at the Upper Boundary	31
3.9	Qualitative Discussion	33
Chapter 4 Finite Elements and the Stokes Problem		35
4.1	Introduction	35
4.2	Variational Formulation	35
4.3	Discretisation	39
4.3.1	Some finite dimensional function spaces	39
4.3.2	A linear algebra problem	43
4.4	Solution of the Linear System	49
Chapter 5 A Numerical Stokes Solver with Error Analysis		50
5.1	A FEniCS-based Glaciological Stokes Solver	50
5.2	Error Analysis	52
5.3	Improvement of Ictools, a FEM Stokes Solver	54
Chapter 6 Conclusion		58
Bibliography		59

List of Figures

	Page
Figure 3.1. The parabolic profile of a gravity-driven viscous flow field with frozen bed.	20
Figure 3.2. Exact velocity, pressure, and basal friction induced by a sticky spot.	34
Figure 4.1. A pressure basis function $\psi_i \in M$ graphed on the edges of a triangular mesh.	40
Figure 4.2. An ordering of vertices and edge midpoints with $n = 16$ and $r = 49$.	41
Figure 4.3. Velocity component basis functions $\phi_{13}, \phi_{45} \in X$	42
Figure 4.4. Sparsity structure of (4.40) augmented by Dirichlet conditions. . . .	46
Figure 4.5. Sparsity structure with both Dirichlet and periodic conditions. . . .	48
Figure 5.1. A numerical Stokes solver in 37 lines using FEniCS.	51
Figure 5.2. Errors in FEM velocity and pressure plotted against maximum element diameter, together with convergence rates m	54
Figure 5.3. \mathbf{H}^1 convergence of velocity using the recommended form (4.22) and the Icetools form (5.4).	56

Acknowledgments

I have been fortunate to have the able assistance of my professors, fellow students, and family while writing this thesis. David Maxwell and John Rhodes served on my committee and made many helpful comments. I thank them for their effective teaching. Ed Bueler provided the right combination of guidance and freedom as my adviser and mentor over the past two years. I thank him for his advice, teaching, and encouragement. Jason Baggett and Odile Bastille, recent graduates of the M.S. program, saved me many hours by providing their expertly formatted class files. My wife, Katie, read several chapters and offered useful writing advice. Thanks, my love, for brightening my dour nature. This work was supported by NASA Modeling, Analysis, and Prediction grant NNX09AJ38G.

Chapter 1

Introduction

The Stokes system of partial differential equations models fluid flows where viscous effects dominate. Examples include the flows of honey, lava, and glaciers as well as the movement of less viscous fluids through confined areas: blood flowing through capillaries and grit settling in engine oil. The purpose of this work is to examine analytical and numerical strategies for solving the Stokes problem in a glaciological context.

Exact solutions are available only in special cases. A 1985 result due to Balise and Raymond gives exact solutions for transient, linear Stokes flow on a rectangle with periodic boundary conditions at the left and right sides, a free surface on top, and a sinusoidal imposed velocity at the base [BR85]. We extend this result by considering arbitrary basal velocities and giving formulas for the pressure and basal shear stress.

The development of numerical simulations capable of approximating nonlinear (*i.e.* variable-viscosity) Stokes flow over realistic geometries is an active area of research in mathematics and glaciology. The linear problem is relevant because many algorithms for the nonlinear problem repeatedly solve the linear one. We describe the use of finite elements in the solution of the linear problem and we present an implementation using the freely-available finite element software package FEniCS. We compare the approximations to exact solutions.

The organization of this thesis is as follows.

In Chapter 2 we give an overview of elementary fluid dynamics for glaciology. We introduce the tensors describing stress and strain and we state constitutive laws relating them. We then derive the Stokes equations and we show how the biharmonic equation arises for the streamfunction that generates planar flows. We discuss boundary conditions and show what special form these conditions take in a rectangular geometry. We conclude with a working definition of Sobolev spaces.

In Chapter 3 we review and extend the results in [BR85]. The first five sections contain results that were stated in that paper and also in the thesis [Jóh92], although the equations appear different because we consider many Fourier terms instead of just one. The material in the remaining sections is new. We provide analytical formulas for the pressure and basal stress and we give a necessary condition on the basal velocities that can be induced by

gravity under the linear (Rayleigh) sliding law on a uniformly sloping bed.

Chapter 4 is an introduction to the finite element method in the context of a glaciological Stokes flow problem. Most tutorials on the finite element method cover a simpler problem such as Poisson's equation. This chapter addresses linear Stokes flow with a zero-stress surface boundary condition at an introductory level.

In Chapter 5 we present a concise implementation of the procedure discussed in Chapter 4. We use the analytical solutions developed in Chapter 3 to analyze the convergence of the numerical simulation. We also discuss and correct an error in a recent published numerical model [Jar08].

Chapter 2

Preliminaries

2.1 Introduction

In this chapter we give an overview of several fundamental topics in viscous fluid flow. In Section 2.2 we define the essential tensor quantities and discuss the equations that relate them. Section 2.3 contains the derivation of the Navier-Stokes and Stokes systems of partial differential equations for incompressible Newtonian fluids. In Section 2.4 we show how the Stokes problem can be reduced to the biharmonic problem in two dimensions. Glaciologically-relevant boundary conditions for Stokes flow are considered in Section 2.5. In Section 2.6 we restate these boundary conditions in the special case of a rectangular geometry, and then translate them for the biharmonic problem. In Section 2.7 we briefly introduce Sobolev spaces, which are fundamental to the modern theory of differential equations.

Three books [Wor09, Goo82, Ach90] were most helpful while I was learning the material of sections 2.2 and 2.3. The first is a brief introduction, extremely well written, striking a good balance between a moderate pace and interesting observations and problems. The others are more comprehensive and I found it helpful to read them simultaneously, especially in their derivations of the Navier-Stokes equations. Another commonly cited reference, which I have not read, is [Bat00].

Many equations in vector calculus are greatly simplified by Einstein's notation for sums of products. If a_1, a_2, \dots, a_n and b_1, b_2, \dots, b_n are scalars then we write

$$a_i b_i := \sum_{i=1}^n a_i b_i = \mathbf{a} \cdot \mathbf{b}. \quad (2.1)$$

That is, repetition of an index in a product implies summation over that index. If σ is an $n \times n$ matrix then $\sigma_{ii} = \sigma_{11} + \sigma_{22} + \dots + \sigma_{nn} = \text{Tr } \sigma$. A vector-matrix-vector product can be conveniently represented as $a_i \sigma_{ij} b_j = \mathbf{a} \sigma \mathbf{b}$, and we avoid the bother of distinguishing row vectors from column vectors in the formulas.

A generalization of the convention includes "products" with derivative operators. For

example, the Divergence Theorem can be written as either

$$\int_{\Omega} \nabla \cdot \mathbf{f} = \int_{\partial\Omega} \mathbf{f} \cdot \mathbf{n} \quad \text{or} \quad \int_{\Omega} \frac{\partial f_i}{\partial x_i} = \int_{\partial\Omega} n_i f_i. \quad (2.2)$$

This convention is very useful for vector and tensor integration by parts.

2.2 Elementary Fluid Dynamics

In this section we introduce the three most important tensors of elementary fluid dynamics: stress, deviatoric stress, and rate of strain. We then discuss the constitutive laws that relate them. We will begin by studying the forces at work within a moving fluid.

2.2.1 Stress, pressure, and deviatoric stress

Suppose that a fluid occupies some open region $\Omega \subseteq \mathbb{R}^3$, and let P be a point within Ω . Let \mathbf{n} be a unit vector at P and let δA be an area element containing P in the plane to which \mathbf{n} is normal. It may be helpful to think of δA as a disk with center P . The fluid into which \mathbf{n} points exerts a force on δA . The ratio of that force to the area of δA is called the *stress* and written $\Sigma(\mathbf{n})$. This quantity depends on the point P and the direction of \mathbf{n} but not on the area of δA if we assume that δA is sufficiently small ([Goo82], chapter 6). In the absence of viscous effects, the stress is in the direction of $-\mathbf{n}$. Viscous fluids in motion generally exert tangential stresses as well.

The map carrying the vector \mathbf{n} to the vector $\Sigma(\mathbf{n})$ is linear; such maps are called *tensors*. In Cartesian coordinates with respect to an orthonormal basis $\{\mathbf{e}_1, \mathbf{e}_2, \mathbf{e}_3\}$, tensors are conveniently represented by matrices. Because we will use the Cartesian system exclusively, we identify all tensors with their matrices. We let σ be the matrix of the tensor $\mathbf{n} \mapsto \Sigma(\mathbf{n})$:

$$\Sigma(\mathbf{n}) = \begin{bmatrix} \sigma_{11} & \sigma_{12} & \sigma_{13} \\ \sigma_{21} & \sigma_{22} & \sigma_{23} \\ \sigma_{31} & \sigma_{32} & \sigma_{33} \end{bmatrix} \begin{bmatrix} n_1 \\ n_2 \\ n_3 \end{bmatrix} = \sigma_{ij} n_j. \quad (2.3)$$

The matrix σ is called the *Cauchy stress tensor* or sometimes just the *stress tensor*; it is a continuous function of the position P . The components of σ have physical meaning. The best way to see this is by taking $\mathbf{n} = \mathbf{e}_i$ in (2.3); we see that the i -th column of σ is the

stress on an area element with normal \mathbf{e}_i . We state without proof the useful fact that σ is a symmetric matrix ([Goo82], chapter 6).

We can now use the Cauchy stress tensor to give a mechanical definition of pressure. For fluids at rest there are no viscous effects and so the off-diagonal elements of σ vanish. Moreover, the magnitude of $\Sigma(\mathbf{n})$ does not depend on the direction of \mathbf{n} and so the diagonal entries of σ are equal. We write $\sigma = -pI$, where p is a scalar and I is the identity matrix. To generalize this to moving fluids we define the pressure p as

$$p = \frac{-1}{d} \sigma_{ii}, \quad (2.4)$$

where d is the dimension of the space (we take $d = 3$ for now).

We now decompose the stress tensor additively by

$$\sigma = -pI + \tau. \quad (2.5)$$

Note that the trace of τ is $\sigma_{ii} + dp = 0$. This decomposition of σ as the sum of a trace-free part and a multiple of I is unique. We say that τ is the *deviatoric stress tensor* because it induces volume-preserving shears and rotations. The pressure term $-pI$ accounts for the isotropic stresses that induce dilation and compression in compressible fluids.

2.2.2 The strain rate tensor

We now abandon our discussion of stress and examine a tensor that describes the spatial variations in the velocity. Let \mathbf{u} be a velocity field. Then $\nabla\mathbf{u}$ is a tensor whose components are given by

$$(\nabla\mathbf{u})_{ij} = \frac{\partial u_j}{\partial x_i}. \quad (2.6)$$

We decompose $\nabla\mathbf{u}$ into symmetric and antisymmetric parts:

$$\nabla\mathbf{u} = \frac{1}{2}(\nabla\mathbf{u} + \nabla\mathbf{u}^T) - \frac{1}{2}(\nabla\mathbf{u}^T - \nabla\mathbf{u}) \quad (2.7)$$

$$= \dot{\epsilon} - \xi. \quad (2.8)$$

The symmetric part $\dot{\epsilon}$ is called the *strain rate tensor*. The antisymmetric part ξ is not needed in our discussion. Because $\dot{\epsilon}$ is real and symmetric it is diagonalizable, i.e. has real eigenvalues corresponding to orthogonal eigenvectors. The eigenvalues quantify the variation of velocity of the fluid in the directions of the eigenvectors. One consequence is that the fluid is compressed or dilated according to the sign of $\dot{\epsilon}_{ii}$; if this vanishes then $\nabla \cdot \mathbf{u} = 0$ and we say that the fluid is *incompressible*.

2.2.3 Constitutive laws

There is no universal law determining the deformation rates of fluids under stress. Air, water, oil, syrup, blood, and ice all respond in different ways to a given applied force. For each fluid we may attempt to model these responses with an equation called a *constitutive law* relating τ to $\dot{\epsilon}$. For incompressible *Newtonian fluids* such as water, the constitutive law is a proportionality relation

$$\tau = 2\mu\dot{\epsilon}. \quad (2.9)$$

and the proportionality constant μ is called the *viscosity* of the fluid.

Glacier ice is a non-Newtonian fluid and requires a more complicated constitutive law. Its acceleration depends in a highly nonlinear way on the stress. It also depends on the size and orientation of the ice crystals, the presence of impurities, the temperature, and the amount of liquid water present. The effective viscosity defined by the elementwise ratio $\tau_{ij}/(2\dot{\epsilon}_{ij})$ varies widely. A range of 10^{13} to 10^{17} Pa·sec is plausible for conditions on Earth (see figure 4.6 in [GB09]). A widely used model that corresponds well to field observations is the *generalized Glen's Law*, which states that the viscosity of glacier ice is inversely proportional to some power of the stress. That is, the glacier ice flows more easily under high deviatoric stresses. To state the law precisely, we define the scalars $\|\dot{\epsilon}\|$ and $\|\tau\|$ by

$$\|\dot{\epsilon}\| = \sqrt{\frac{1}{2}\dot{\epsilon}_{ij}\dot{\epsilon}_{ij}}, \quad \|\tau\| = \sqrt{\frac{1}{2}\tau_{ij}\tau_{ij}}, \quad (2.10)$$

then make the assumption

$$\|\dot{\epsilon}\| = A\|\tau\|^n, \quad (2.11)$$

and finally replace μ in (2.9) by the effective viscosity

$$\eta = \frac{1}{2}(A \|\tau\|^{n-1})^{-1} \quad (2.12)$$

$$= \frac{1}{2}A^{-1/n} \|\dot{\epsilon}\|^{(1-n)/n}. \quad (2.13)$$

Here A is a scalar called the *ice softness* depending strongly on temperature and on the crystal size. The exponent n is a constant usually taken equal to 3, although observations of n in the literature range from 1.5 to 4 ([CP10], p.55). In particular, n appears to be somewhat smaller than 3 for low stresses.

This flow law is sophisticated but still has shortcomings. Even if we include some thermodynamics by employing a non-constant creep parameter – an effort not undertaken in some current published models such as [LJG⁺12] – this generalized flow law fails to take into account the phenomenon of *anisotropy*, the dependence of fluid response on the direction of an applied stress. This occurs when ice crystals align in some large region of ice, which then deforms more easily along one plane of the crystal structure.

In this paper we will mostly take $n = 1$, which reduces Glen’s Law to the Newtonian case (2.9). There are good reasons to investigate the behavior of a Newtonian ice sheet, despite its poor resemblance to an actual ice sheet. In particular, the widely used *Picard iteration* for approximating nonlinear flows requires solving a linear problem repeatedly [LJG⁺12, Jar08].

2.3 The Navier-Stokes and Stokes Equations

Newton’s Second Law states that the force on an object is equal to the product of its mass and its acceleration. We now apply this observation to a hypothetical blob occupying a region Ω within a fluid. The blob may move, so we let $\Omega = \Omega(t)$ depend on time.

The forces acting on the blob include a surface force exerted by the surrounding fluid as well as a body force acting on all fluid particles. The surface force is a vector given by the surface integral of the stress tensor, which we write as a volume integral using the Divergence Theorem. In component form this reads

$$\int_{\partial\Omega} \sigma_{ij} n_j = \int_{\Omega} \frac{\partial \sigma_{ij}}{\partial x_j}. \quad (2.14)$$

while in vector form it is instead written

$$\int_{\partial\Omega} \boldsymbol{\sigma} \cdot \mathbf{n} = \int_{\Omega} \nabla \cdot \boldsymbol{\sigma}. \quad (2.15)$$

For the vector equation we are using the possibly unfamiliar definition of the tensor divergence

$$\nabla \cdot T = \frac{\partial T_{ij}}{\partial x_j}, \quad (2.16)$$

as well as the convention that the integral of a vector field is the vector obtained by integration in each component. The only important body force for glaciological applications is that caused by gravity; see Chapter 5 of [GB09] for an argument that Coriolis forces can be neglected even for continental-scale models. The body force is therefore given by

$$\int_{\Omega} \rho \mathbf{g}$$

where ρ is the constant density and $\mathbf{g} = (0, 0, -9.81 \text{ m/sec}^2)$ in the usual 3-dimensional basis.

Having described the forces acting on our blob of fluid, we now write down the rate of change of momentum, or the product of mass and acceleration. If the velocity field is \mathbf{u} , the momentum of the blob is the vector

$$\int_{\Omega} \rho \mathbf{u}.$$

To describe the rate of change of the momentum, we must be careful to distinguish between the quantities

$$\frac{\partial}{\partial t} \int_{\Omega(t_0)} \rho \mathbf{u}(t) \quad \text{and} \quad \frac{\partial}{\partial t} \int_{\Omega(t)} \rho \mathbf{u}(t).$$

The first gives the rate of change of the momentum of the fluid occupying a fixed region of space, while the second gives the rate of change of the momentum of a fixed blob of the fluid moving through space. The second quantity is appropriate for our moving blob, and so $\int_{\Omega(t_0)} \rho \frac{\partial}{\partial t} \mathbf{u}(t)$ is unsuitable for describing the rate of change of momentum. We therefore introduce an operator $\frac{D}{Dt}$ called the *derivative following the fluid* or *material derivative*.

Let $\mathbf{x}(t)$ parameterize the position of a particle traveling according to a time-dependent velocity field $\mathbf{u}(t)$, i.e. $\frac{\partial}{\partial t}x_i(t) = u_i(t)$. For a scalar quantity f depending on position and time, we define

$$\frac{Df}{Dt} = \frac{\partial}{\partial t}f(\mathbf{x}, t) = \frac{\partial f}{\partial t} + \frac{\partial f}{\partial x_i} \frac{\partial x_i}{\partial t} = \frac{\partial f}{\partial t} + \frac{\partial f}{\partial x_i} u_i = \frac{\partial f}{\partial t} + (\nabla f) \cdot \mathbf{u}. \quad (2.17)$$

The rate of change of momentum of the moving blob at a given time $t = t_0$ now becomes

$$\left. \frac{\partial}{\partial t} \right|_{t=t_0} \int_{\Omega(t)} \rho \mathbf{u}(t) = \int_{\Omega(t_0)} \rho \frac{D\mathbf{u}(t_0)}{Dt}; \quad (2.18)$$

see [Ach90] for details.

We now set the rate of change of momentum equal to the sum of the applied forces. This gives

$$\int_{\Omega} \rho \frac{D\mathbf{u}}{Dt} = \int_{\Omega} \nabla \cdot \boldsymbol{\sigma} + \int_{\Omega} \rho \mathbf{g}. \quad (2.19)$$

Because the region Ω defining the blob was arbitrary, the integrands must be equal:

$$\rho \frac{D\mathbf{u}}{Dt} = \nabla \cdot \boldsymbol{\sigma} + \rho \mathbf{g} \quad (2.20)$$

$$= \nabla \cdot \boldsymbol{\tau} - \nabla p + \rho \mathbf{g}. \quad (2.21)$$

Equation (2.21) is the famous Navier-Stokes equation. A standard form uses $\frac{D\mathbf{u}}{Dt} = \frac{\partial \mathbf{u}}{\partial t} + (\nabla \mathbf{u}) \cdot \mathbf{u}$.

In a glaciological context, we instead make the approximation $\frac{D\mathbf{u}}{Dt} = 0$. To see that this approximation is reasonable, we can compare the relative magnitudes of the vectors ∇p and $\rho \frac{D\mathbf{u}}{Dt}$ at realistic values of the parameters. Greve and Blatter [GB09] take

$$\begin{aligned} \text{horizontal extent} \quad L &= 1000 \text{ km}, \\ \text{vertical extent} \quad H &= 1 \text{ km}, \\ \text{horizontal velocity} \quad U &= 100 \text{ m/a}, \\ \text{vertical velocity} \quad W &= 0.1 \text{ m/a}, \\ \text{pressure} \quad P &= \rho g H \approx 10^7 \text{ Pa}, \\ \text{time-scale} \quad t &= L/U = H/W = 10^4 \text{ a}, \end{aligned} \quad (2.22)$$

for an ice sheet. The ratio of $\rho \frac{D\mathbf{u}}{Dt}$ to ∇p , known as the Froude number, is given for the horizontal direction by

$$Fr = \frac{\rho U/t}{P/L} = \frac{\rho U^2/L}{\rho g H/L} = \frac{U^2}{gH}. \quad (2.23)$$

Expressing U^2 using seconds instead of years, we obtain the quantity $U^2 = 10^4/(3600 \times 24 \times 365.251)^2 \approx 10^4 \times 10^{-15}$. Dividing by $g \approx 10$ and $H = 1000$ we find $Fr \approx 10^{-21}$. A similar comparison in the vertical direction gives an even smaller ratio $\approx 10^{-21}$. There may be unrealistic assumptions in our models, but the approximation $\frac{D\mathbf{u}}{Dt} = 0$ is harmless for physically realistic ice flow scenarios on Earth.

The combination of this *Stokes equation* and incompressibility forms the *Stokes system* of partial differential equations

$$\mathbf{0} = \nabla \cdot \boldsymbol{\sigma} + \rho \mathbf{g}, \quad (2.24)$$

$$\mathbf{0} = \nabla \cdot \mathbf{u}. \quad (2.25)$$

Mathematics books refer to this system as the *steady Stokes equations*. It is often written in terms of velocity and pressure:

$$-\mu \Delta \mathbf{u} + \nabla p = \rho \mathbf{g}, \quad (2.26)$$

$$\nabla \cdot \mathbf{u} = 0. \quad (2.27)$$

We now demonstrate the equivalence of these systems in the Newtonian case where $\boldsymbol{\tau} = 2\mu \dot{\boldsymbol{\epsilon}}$. To express $\boldsymbol{\sigma}$ in terms of \mathbf{u} and p , recall that $\boldsymbol{\sigma} = \boldsymbol{\tau} - p\mathbf{I}$ so that $\nabla \cdot \boldsymbol{\sigma} = \nabla \cdot \boldsymbol{\tau} - \nabla p$. We also recall that $\dot{\boldsymbol{\epsilon}} = \frac{1}{2}(\nabla \mathbf{u} + \nabla \mathbf{u}^T)$. This gives

$$\begin{aligned} \nabla \cdot \boldsymbol{\sigma} &= \nabla \cdot \boldsymbol{\tau} + \nabla p \\ &= 2\mu \nabla \cdot \dot{\boldsymbol{\epsilon}} - \nabla p \\ &= \mu \nabla \cdot (\nabla \mathbf{u}) + \mu \nabla \cdot (\nabla \mathbf{u}^T) - \nabla p. \end{aligned} \quad (2.28)$$

The first term vanishes; indeed $\nabla \cdot (\nabla \mathbf{u}) = \frac{\partial}{\partial x_j} \frac{\partial u_j}{\partial x_i} = \frac{\partial}{\partial x_i} (\nabla \cdot \mathbf{u}) = 0$. The second term is the desired Laplacian since $\nabla \cdot (\nabla \mathbf{u}^T) = \frac{\partial}{\partial x_j} \frac{\partial u_i}{\partial x_j} = \Delta \mathbf{u}$. Hence $\nabla \cdot \boldsymbol{\sigma} = \mu \Delta \mathbf{u} - \nabla p$ as desired.

2.4 The Biharmonic Equation

In the two-dimensional or planar flow case, the Stokes system in the form (2.26) is stated in terms of three functions: the pressure and the two components of velocity. In this section we introduce the concept of a streamfunction and show that this reduces the Stokes system to a simpler partial differential equation, namely the biharmonic equation, stated in terms of the stream function alone. This will enable us to provide analytical solutions in Chapter 3.

It is a theorem in vector calculus that if the divergence of a vector field \mathbf{u} vanishes in a simply connected region, then \mathbf{u} is the curl of some vector field A . In the two-dimensional case $\mathbf{u} = (u, 0, w)$, the function A may be assumed to have the form $A = (0, \psi(x, z), 0)$. Hence there is a real-valued *streamfunction* $\psi(x, z)$ such that

$$u = \frac{\partial \psi}{\partial z}; \quad w = -\frac{\partial \psi}{\partial x}. \quad (2.29)$$

We now divide (2.26) by μ and take the curl, which eliminates the gradients ∇p and $\rho \mathbf{g}$:

$$0 = \nabla \times \left(\Delta \mathbf{u} - \frac{1}{\mu} \nabla p + \frac{\rho}{\mu} \mathbf{g} \right) \quad (2.30)$$

$$= \nabla \times \left(\Delta \left(\frac{\partial \psi}{\partial z}, 0, -\frac{\partial \psi}{\partial x} \right) \right) + 0 + 0 \quad (2.31)$$

$$= \nabla \times \left(\frac{\partial^3 \psi}{\partial x^2 \partial z} + \frac{\partial^3 \psi}{\partial z^3}, 0, -\frac{\partial^3 \psi}{\partial x^3} - \frac{\partial^3 \psi}{\partial x \partial z^2} \right) \quad (2.32)$$

$$= \left(0, \frac{\partial^4 \psi}{\partial x^4} + \frac{\partial^4 \psi}{\partial x^2 \partial z^2} + \frac{\partial^4 \psi}{\partial z^2 \partial x^2} + \frac{\partial^4 \psi}{\partial z^4}, 0 \right) \quad (2.33)$$

so that

$$0 = \Delta \Delta \psi. \quad (2.34)$$

This is the *biharmonic equation*, which also arises in the context of measuring the deflection of metal plates or beams under a given load. We have shown that if \mathbf{u} is a velocity field satisfying (2.26), then a streamfunction satisfying (2.29) is biharmonic. In the next chapter we will obtain analytical solutions for the Stokes equations by solving the biharmonic equation.

2.5 General Boundary Conditions for Glaciology

We complete our boundary value problem by choosing glaciologically-relevant boundary conditions.

We begin with the ice-atmosphere boundary. It is reasonable to assume the atmosphere exerts no normal force at the top of an ice sheet; atmospheric pressure is insignificant compared with typical pressures under hundreds of meters of ice. That is,

$$\mathbf{n} \cdot \boldsymbol{\sigma} \cdot \mathbf{n} = 0. \quad (2.35)$$

We also assume that the atmosphere exerts no tangential force on the surface, *i.e.* wind blowing across the surface of a glacier will not alter the flow in a meaningful way:

$$\boldsymbol{\sigma} \cdot \mathbf{n} - (\mathbf{n} \cdot \boldsymbol{\sigma} \cdot \mathbf{n})\mathbf{n} = 0. \quad (2.36)$$

These equations are equivalent to

$$\boldsymbol{\sigma} \cdot \mathbf{n} = 0. \quad (2.37)$$

In some situations it may be necessary to write this condition in terms of \mathbf{u} and p instead of $\boldsymbol{\sigma}$. We will do this in the next section when we specialize to a rectangular geometry.

The simplest condition that may be imposed on the lower boundary is the no-slip condition $\mathbf{u} = \mathbf{0}$. In the next chapter we consider a generalization where the horizontal component is arbitrary: $\mathbf{u} = (u, w) = (f, 0)$. In practice, the basal velocities of glaciers are unknown and so we must search for alternatives. One of the simplest of these is the *linear sliding law* given by the equations

$$\mathbf{u} \cdot \mathbf{n} = 0, \quad (2.38)$$

$$\mathbf{n} \cdot \boldsymbol{\sigma} \cdot \mathbf{t} = -\beta^2 \mathbf{u} \cdot \mathbf{t} \quad (2.39)$$

where \mathbf{n} is the outward unit normal vector and \mathbf{t} is any vector tangential to the boundary. The *impermeability condition* (2.38) implies that there is no flow into or out of the base. The second condition (2.39) relates the tangential component of the stress exerted by the ice on the base to the slip rate. If the parameter β^2 is increased, then a given slip rate

requires a larger stress. Therefore β^2 can be understood as a friction coefficient.

If our goal is to model a mountain glacier whose terminus is on dry ground, then the upper and lower surfaces meet and there are no other boundaries to consider. If we wish to model only a section of a glacier or ice sheet, we must consider inflow and outflow at the lateral boundaries Γ_l and Γ_r . If the shapes of these boundaries are similar we can use periodic conditions such as

$$\mathbf{u}|_{\Gamma_l} = \mathbf{u}|_{\Gamma_r}, \quad \text{and} \quad \left. \frac{\partial \mathbf{u}}{\partial x_1} \right|_{\Gamma_l} = \left. \frac{\partial \mathbf{u}}{\partial x_1} \right|_{\Gamma_r}. \quad (2.40)$$

We do not consider the alternate scenarios of calving and/or ice shelves.

2.6 Boundary Conditions in the Rectangular Case

We now restrict our attention to the case of two-dimensional or planar flow on a rectangular domain Ω . We consider $\Omega = [0, L] \times [0, H]$ with the origin at the lower left corner. We rotate the rectangle and our axes through an angle of $-\alpha$ so that the force \mathbf{g} due to gravity is given by the vector

$$\mathbf{g} = (g_1, g_2) = (g\rho \sin(\alpha), -g\rho \cos(\alpha)). \quad (2.41)$$

In this special geometry the boundary conditions of the previous section can be expressed differently. We describe each of these conditions in terms of \mathbf{u} and p and then derive equivalent formulations for the stream function.

We begin with the stress-free condition $\sigma \cdot \mathbf{n} = 0$. The first step is to express σ in terms of velocity and pressure. Using the equations $\sigma = -pI + \tau$ and $\tau = 2\mu\dot{\epsilon}$, the boundary condition becomes

$$(-pI + 2\mu\dot{\epsilon}) \cdot \mathbf{n} = 0 \quad (2.42)$$

or, with $\mathbf{n} = (0, 1)$ and in matrix form,

$$\begin{bmatrix} -p + 2\mu \frac{\partial u_1}{\partial x_1} & \mu \left(\frac{\partial u_1}{\partial x_2} + \frac{\partial u_2}{\partial x_1} \right) \\ \mu \left(\frac{\partial u_2}{\partial x_1} + \frac{\partial u_1}{\partial x_2} \right) & -p + 2\mu \frac{\partial u_2}{\partial x_2} \end{bmatrix} \begin{bmatrix} 0 \\ 1 \end{bmatrix} = \begin{bmatrix} 0 \\ 0 \end{bmatrix}. \quad (2.43)$$

This gives a pair of equations

$$\frac{\partial u_1}{\partial x_2} + \frac{\partial u_2}{\partial x_1} = 0, \quad (2.44)$$

$$2\mu \frac{\partial u_2}{\partial x_2} = p. \quad (2.45)$$

It is now convenient to change our notation, writing $\mathbf{u} = (u, w)$ instead of $\mathbf{u} = (u_1, u_2)$ and renaming variables $x = x_1$ and $z = x_2$. We can then write u_z instead of $\frac{\partial u_1}{\partial x_2}$, etc. The previous equations become

$$u_z + w_x = 0, \quad (2.46)$$

$$2\mu w_z = p. \quad (2.47)$$

The pressure appearing in the second equation can be converted back to velocity through the Stokes equation, $\nabla p = \mu \Delta \mathbf{u} + \mathbf{g}$. This is a vector equation whose two scalar components read

$$p_x = \mu(u_{xx} + u_{zz}) + g_1, \quad (2.48)$$

$$p_z = \mu(w_{xx} + w_{zz}) + g_2. \quad (2.49)$$

Because (2.47) holds on the upper surface $\{(x, H) : x \in [0, L]\}$, we can differentiate it with respect to x (but not z) and eliminate the pressure derivative through (2.48). The result is a non-homogeneous boundary condition

$$2\mu w_{zx} = \mu(u_{xx} + u_{zz}) + g_1. \quad (2.50)$$

We now write the free-surface boundary conditions (2.46) and (2.50) in terms of the stream function ψ . Recalling that $u = \psi_z$ and $w = -\psi_x$, we have the conditions

$$\psi_{zz} - \psi_{xx} = 0, \quad (2.51)$$

$$-2\mu\psi_{xzx} = \mu(\psi_{zxx} + \psi_{zzz}) + g_1. \quad (2.52)$$

Simplifying these we obtain

$$\psi_{zz} - \psi_{xx} = 0, \quad (2.53)$$

$$3\psi_{xxz} + \psi_{zzz} = -g_1/\mu. \quad (2.54)$$

These are the boundary conditions that we seek to enforce on the free surface in the biharmonic problem.

On the base we impose a velocity profile $(u, w) = (f, 0)$, where $f(0) = f(L)$. Written in terms of ψ , this becomes

$$\psi_z = f \text{ on } [0, L] \times 0, \quad (2.55)$$

$$\psi_x = 0 \text{ on } [0, L] \times 0. \quad (2.56)$$

In this problem we are interested only in the derivatives of ψ . We may therefore add arbitrary constants to ψ without affecting the derived velocity solution. Because (2.56) implies that ψ is constant on the bed, we may without loss of generality assume that $\psi = 0$ on the bed. Hence we seek a solution satisfying

$$\psi_z = f \text{ on } [0, L] \times 0, \quad (2.57)$$

$$\psi = 0 \text{ on } [0, L] \times 0. \quad (2.58)$$

We take periodic boundary conditions on the left and right sides. For the Stokes problem these take the form

$$u(0, z) = u(L, z), \quad (2.59)$$

$$u_x(0, z) = u_x(L, z), \quad (2.60)$$

$$w(0, z) = w(L, z), \quad (2.61)$$

$$w_x(0, z) = w_x(L, z). \quad (2.62)$$

Written in terms of ψ , we have

$$\psi_z(\mathbf{0}, z) = \psi_z(L, z), \quad (2.63)$$

$$\psi_{xz}(\mathbf{0}, z) = \psi_{xz}(L, z), \quad (2.64)$$

$$\psi_x(\mathbf{0}, z) = \psi_x(L, z), \quad (2.65)$$

$$\psi_{xx}(\mathbf{0}, z) = \psi_{xx}(L, z). \quad (2.66)$$

2.7 Sobolev Spaces

Sobolev spaces are fundamental to the modern theory of differential equations because they allow us to construct Banach spaces containing differentiable functions. The completeness of these spaces is a useful tool for proving existence and uniqueness theorems [DM05]. In this work we will omit such proofs, but we give the basic definitions in this section.

Consider the one-dimensional absolute value function $f \in C(-1, 1)$. According to the classical definitions of calculus, f fails to be differentiable at zero and so there is no function $g \in C(-1, 1)$ that we may call the derivative of f . Of course, at all points other than zero the derivative of f is defined and equals $x/|x| = \text{sgn}(x)$.

The theory of *distributions* provides a more accommodating notion of derivative. Let $\Omega \subset \mathbb{R}^n$ be an open set with Lipschitz boundary, and let $\mathcal{D}(\Omega)$ be the set of infinitely differentiable functions with compact support contained in Ω . Then a *distribution* is a continuous linear map from $\mathcal{D}(\Omega)$ to \mathbb{R} , where “continuous” means $f(\varphi) = \lim_{n \rightarrow \infty} f(\varphi_n)$ whenever $\left\| \varphi_n^{(m)} - \varphi^{(m)} \right\|_2 \rightarrow 0$ for each m . Taking $\Omega = (-1, 1)$, one example is $\varphi \mapsto \varphi(0)$ and another is given by $\varphi \mapsto \int_{-1}^1 \varphi f$ if $f \in L^2(-1, 1)$. This allows us to identify any L^2 function with a distribution.

The derivative of a distribution g can always be defined by $g'(\varphi) = -g(\varphi')$. In particular, whenever $f \in L^2$ we may view f as a distribution and then find another distribution g that is its derivative. Of course, g is now a distribution and may not coincide with any L^2 function; if it does, we say that $g \in L^2$ is a distributional derivative of f . The qualitative result of this theory is that continuous functions failing to be differentiable on a null set, like the absolute value function, can be said to have derivatives in this distributional sense:

$$\text{sgn} = \text{abs}'.$$

Continuity is important; the sgn function has no distributional derivative. In two dimensions, a function may be discontinuous at a point (but not across a segment) and still have a distributional derivative.

We conclude with one essential definition. The *Sobolev space* $H^1(\Omega)$ is the set of L^2 functions having distributional derivatives in each of the n space directions:

$$H^1(\Omega) = \{f \in L^2 : \partial f / \partial x_i \in L^2 \text{ for } 1 \leq i \leq n\}. \quad (2.67)$$

The space $H^1(\Omega)$ is complete with respect to the norm induced by the inner product

$$\langle f, g \rangle_{H^1} = \int_{\Omega} fg + \int_{\Omega} (\nabla f) \cdot (\nabla g). \quad (2.68)$$

Chapter 3

Exact Solutions

In this chapter we give exact solutions for the Stokes problem in a special case applicable to glaciology. The main result was first given by [BR85] in the case of a single Fourier term for the basal forcing. We modify their proof of that result for the case of many Fourier terms. We then extend [BR85] by giving formulas for the pressure and stress, and we give necessary conditions on basal velocities that can arise under the linear sliding law. A qualitative discussion of the solutions is included.

3.1 The Boundary Value Problem

We consider the Stokes problem on a rectangle $\Omega = [0, L] \times [0, H]$. We rotate the rectangle and our axes through an angle of $-\alpha$ so that the force due to gravity is given by the vector

$$\mathbf{g} = (g_1, g_2) = (g\rho \sin(\alpha), -g\rho \cos(\alpha)). \quad (3.1)$$

We impose an arbitrary basal velocity $\mathbf{u}|_{z=0} = (f, 0)$, periodic conditions at the lateral boundaries, and the stress-free condition at the surface. The boundary value problem can be stated as the search for a velocity $\mathbf{u} = (u, w)$ and pressure p such that

$$\nabla p - \mu \Delta \mathbf{u} = \mathbf{g} \quad \text{on } \Omega \quad (3.2)$$

$$\nabla \cdot \mathbf{u} = 0 \quad \text{on } \Omega, \quad (3.3)$$

$$\mathbf{u}(0, z) - \mathbf{u}(L, z) = \mathbf{0} \quad \text{for all } z, \quad (3.4)$$

$$\left. \frac{\partial \mathbf{u}}{\partial x} \right|_{(0,z)} - \left. \frac{\partial \mathbf{u}}{\partial x} \right|_{(L,z)} = \mathbf{0} \quad \text{for all } z, \quad (3.5)$$

$$(u, w) = (f, 0) \quad \text{on } \{z = 0\}, \quad (3.6)$$

$$\frac{\partial w}{\partial x} + \frac{\partial u}{\partial z} = 0 \quad \text{on } \{z = H\}, \quad (3.7)$$

$$2\mu w_{zx} - \mu(u_{xx} + u_{zz}) = g_1 \quad \text{on } \{z = H\}. \quad (3.8)$$

The upper-surface conditions (3.7) and (3.8) are weaker than the desired stress-free condition (2.37) because we differentiated (2.47) while specializing (2.37) to the rectangular case. As a result, the pressure solution is only determined up to an additive constant in

the system (3.2)-(3.8). In section 3.8 we will determine the correct constant term and show that our solution satisfies the stronger condition (2.37).

The biharmonic boundary value problem obtained from (3.2)-(3.8) by putting $\psi_z = u$, $-\psi_x = w$ is as follows: find a scalar function ψ on Ω such that

$$\Delta\Delta\psi = 0 \quad \text{on } \Omega, \quad (3.9)$$

$$\psi_z(0, z) - \psi_z(L, z) = 0 \quad \text{for all } z, \quad (3.10)$$

$$\psi_{xz}(0, z) - \psi_{xz}(L, z) = 0 \quad \text{for all } z, \quad (3.11)$$

$$\psi_x(0, z) - \psi_x(L, z) = 0 \quad \text{for all } z, \quad (3.12)$$

$$\psi_{xx}(0, z) - \psi_{xx}(L, z) = 0 \quad \text{for all } z, \quad (3.13)$$

$$\psi(x, 0) = 0 \quad \text{for all } x, \quad (3.14)$$

$$\psi_z(x, 0) = f \quad \text{for all } x, \quad (3.15)$$

$$\psi_{zz}(x, H) - \psi_{xx}(x, H) = 0 \quad \text{for all } x, \quad (3.16)$$

$$3\psi_{xxz}(x, H) + \psi_{zzz}(x, H) = -g_1/\mu \quad \text{for all } x. \quad (3.17)$$

There are two nonhomogeneous conditions (3.15) and (3.17). Because the problem is linear, we will solve the two simpler problems obtained by setting their right-hand sides to zero in turn and then add the two solutions. These solutions have physical meaning. The first, with (3.15) set to zero, represents gravity driven flow with a no-slip condition at the glacier bed. The second represents a flow driven by basal forcing in the absence of gravity.

3.2 The No-Slip Case

The biharmonic problem (3.9)- (3.17) with (3.15) replaced by $\psi_z(x, 0) = 0$ has a surprisingly simple solution. Indeed, the reader should verify that

$$\Psi_1(x, z) = \frac{g_1 H}{2\mu} z^2 - \frac{g_1}{6\mu} z^3 \quad (3.18)$$

solves the system. It is useful to find the velocity field arising from this stream function. The vertical component is $w = -\psi_x = 0$, so the flow is parallel, and for the horizontal

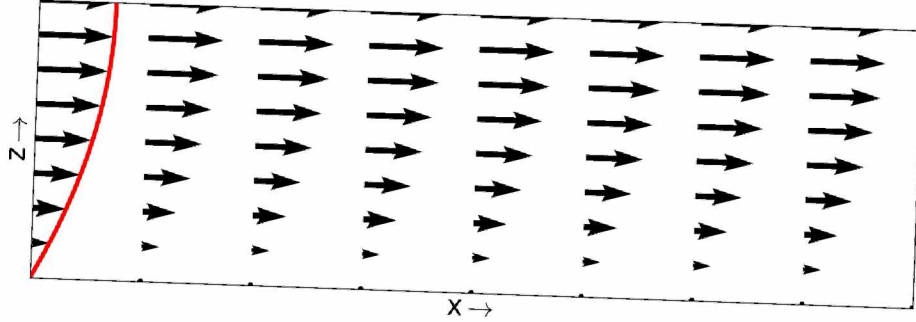


Figure 3.1. The parabolic profile of a gravity-driven viscous flow field with frozen bed.

component we find a parabolic profile

$$u(x, z) = \psi_z(x, z) = \frac{g_1 H}{\mu} z - \frac{g_1}{2\mu} z^2. \quad (3.19)$$

This formula agrees with equation (2.19) in [Ach90]; we have recovered the well-known exact solution known as *laminar flow*. We note that (3.19) is reasonable qualitatively: horizontal flow is proportional to the horizontal component of gravity and inversely proportional to viscosity. The velocity field is depicted in Figure 3.1 for a 40 km section of a glacier of thickness 1 km. With a slope angle of 2° and viscosity 10^{14} Pa · s we obtain a surface speed of 52.2 meters per year.

3.3 The No-Gravity Case

We now consider the case where $g = 0$ and $f \neq 0$. This requires more work and we divide the effort into several subsections.

3.3.1 Reduction to an ordinary differential equation

Our first goal is to identify a collection of separated solutions of the biharmonic equation whose x -components are periodic and form a complete basis for $L^2([0, L])$. A natural choice is to seek solutions of the form $\psi(x, z) = X(x)Z(z)$ where the function $X(x)$ belongs to the collection

$$\mathcal{B} = \left\{ \sin\left(\frac{2\pi n}{L}x\right) \right\}_{n=1}^{\infty} \cup \left\{ \cos\left(\frac{2\pi n}{L}x\right) \right\}_{n=0}^{\infty}. \quad (3.20)$$

If $X \in \mathcal{B}$ then we have $X'' = -\lambda^2 X$ and $X^{(iv)} = \lambda^4 X$, where $\lambda = \frac{2\pi n}{L}$ for some nonnegative integer n . The biharmonic equation then has the form

$$0 = \Delta\Delta\psi = X^{(iv)}Z + 2X''Z'' + XZ^{(iv)} \quad (3.21)$$

$$= X \cdot [\lambda^4 Z - 2\lambda^2 Z'' + Z^{(iv)}]. \quad (3.22)$$

We will therefore seek functions $Z(z)$ solving the ordinary differential equation

$$0 = \lambda^4 Z - 2\lambda^2 Z'' + Z^{(iv)}. \quad (3.23)$$

We consider the cases $\lambda = 0$ and $\lambda > 0$ separately.

3.3.2 Nonzero eigenvalues

For positive λ , (3.23) is a constant-coefficient ordinary differential equation with characteristic polynomial

$$(y^2 - \lambda^2)^2 = 0. \quad (3.24)$$

There are two roots $\pm\lambda$, each of multiplicity two, and so the standard theory of ODEs gives the general solution:

$$Z(z) = a \exp(\lambda z) + b \exp(-\lambda z) + cz \exp(\lambda z) + dz \exp(-\lambda z). \quad (3.25)$$

We will be enforcing boundary conditions at $z = 0$ and $z = H$, so we choose to expand the solution in a more convenient basis:

$$Z(z) = a \sinh(\lambda z) + b \cosh(\lambda z) + cz \sinh(\lambda(z - H)) + dz \cosh(\lambda(z - H)). \quad (3.26)$$

We now use the boundary conditions (3.14), (3.16), and (3.17) to write b, c , and d in terms of a . (3.14) immediately implies that $Z(0) = 0$ and so $b = 0$. The remaining conditions

involve three derivatives of Z . We list them here, for reference:

$$\begin{aligned} Z'(z) &= \lambda a \cosh(\lambda z) + c \sinh(\lambda(z - H)) + d \cosh(\lambda(z - H)) \\ &\quad + \lambda cz \cosh(\lambda(z - H)) + \lambda dz \sinh(\lambda(z - H)), \end{aligned} \quad (3.27)$$

$$\begin{aligned} Z''(z) &= \lambda^2 a \sinh(\lambda z) + 2\lambda c \cosh(\lambda(z - H)) + 2\lambda d \sinh(\lambda(z - H)) \\ &\quad + \lambda^2 cz \sinh(\lambda(z - H)) + \lambda^2 dz \cosh(\lambda(z - H)), \end{aligned} \quad (3.28)$$

$$\begin{aligned} Z'''(z) &= \lambda^3 a \cosh(\lambda z) + 3\lambda^2 c \sinh(\lambda(z - H)) + 3\lambda^2 d \cosh(\lambda(z - H)) \\ &\quad + \lambda^3 cz \cosh(\lambda(z - H)) + \lambda^3 dz \sinh(\lambda(z - H)). \end{aligned} \quad (3.29)$$

Because $X''(x) = -\lambda^2 X(x)$, the conditions (3.16) and (3.17) become

$$Z''(H) + \lambda^2 Z(H) = 0, \quad (3.30)$$

$$-3\lambda^2 Z'(H) + Z'''(H) = 0. \quad (3.31)$$

On substituting the preceding formula for Z'' into (3.30) we obtain

$$(\lambda^2 a \sinh(\lambda H) + 2\lambda c + \lambda^2 dH) + \lambda^2(a \sinh(\lambda H) + dH) = 0. \quad (3.32)$$

Simplifying and dividing by 2λ , this gives one linear equation in a , c , and d :

$$0 = a\lambda \sinh(\lambda H) + \lambda dH + c. \quad (3.33)$$

Similarly, the second condition (3.31) implies that

$$\lambda^3 a \cosh(\lambda H) + 3\lambda^2 d + \lambda^3 cH = 3\lambda^2[\lambda a \cosh(\lambda H) + d + \lambda cH]. \quad (3.34)$$

Canceling $3\lambda^2 d$, moving all terms to the right, and dividing by $2\lambda^3$ we obtain

$$0 = cH + a \cosh(\lambda H)$$

so that

$$c = \frac{-a}{H} \cosh(\lambda H). \quad (3.35)$$

This lets us eliminate c from (3.33) and so we can write d as a multiple of a :

$$d = \frac{a}{\lambda H} \left[\frac{1}{H} \cosh(\lambda H) - \lambda \sinh(\lambda H) \right]. \quad (3.36)$$

We have determined $Z(z)$ up to multiplication by an arbitrary constant a :

$$Z(z) = \sinh(\lambda z) - \frac{\cosh(\lambda H)}{H} z \sinh(\lambda(z - H)) + \left(\frac{\cosh(\lambda H)}{\lambda H^2} - \frac{\sinh(\lambda H)}{H} \right) z \cosh(\lambda(z - H)). \quad (3.37)$$

Notice that this formula is symmetric in the sense that replacing λ with $-\lambda$ has the effect of multiplying $Z(z)$ by -1 . This symmetry is expected since the characteristic polynomial (3.24) has the same property. As a result we do not have to consider $\lambda < 0$.

3.3.3 The zero eigenvalue

The case $\lambda = 0$ corresponds to the choice $X(x) = 1$. In this case (3.23) reduces to $Z^{(iv)} = 0$. This implies that $Z(z)$ is a cubic polynomial, so the streamfunction has the form

$$\psi(x, z) = Z(z) = a + bz + cz^2 + dz^3. \quad (3.38)$$

Now all terms with derivatives in the x -direction vanish from the boundary conditions (3.16) and (3.17). Thus $Z(z)$ satisfies

$$Z(0) = 0, Z''(H) = 0, Z'''(H) = 0.$$

The first condition gives $a = 0$ and the last gives $d = 0$. Then $0 = Z''(H) = 2c$ and $c = 0$ as well. Hence the zero eigenvalue gives a streamfunction

$$\psi(x, z) = bz \quad (3.39)$$

where b is arbitrary.

3.3.4 The nonhomogeneous boundary condition

We now seek to satisfy the condition (3.15) by forming an appropriately-weighted sum of the eigenfunctions we have identified. Let

$$f = a_0 + \sum_{n=1}^{\infty} a_n \sin(\lambda_n x) + b_n \cos(\lambda_n x) \quad (3.40)$$

be the Fourier expansion of f . Define $\psi_0(x, z) = a_0 z$ and for each $n \in \mathbb{N}$ define

$$\psi_n(x, z) = [A_n \sin(\lambda_n x) + B_n \cos(\lambda_n x)] Z_n(z) \quad (3.41)$$

where Z_n is defined by putting $\lambda = \lambda_n$ in (3.37), and A_n and B_n are defined by

$$A_n = a_n \cdot \frac{\lambda_n H^2}{\lambda_n^2 H^2 + \cosh^2(\lambda_n H)} \quad (3.42)$$

$$B_n = b_n \cdot \frac{\lambda_n H^2}{\lambda_n^2 H^2 + \cosh^2(\lambda_n H)}. \quad (3.43)$$

These choices of A_n and B_n are justified by the following calculation of $\frac{\partial \psi_n}{\partial z} \Big|_{z=0}$. For $n = 0$ we have

$$\frac{\partial \psi_0}{\partial z}(x, 0) = a_0 \quad (3.44)$$

and for $n > 0$ we have

$$\frac{\partial \psi_n}{\partial z}(x, 0) = [A_n \sin(\lambda_n x) + B_n \cos(\lambda_n x)] Z_n'(0). \quad (3.45)$$

To obtain a formula for Z_n' we substitute the values of c and d given by (3.35) and (3.36) into (3.27). This gives

$$\begin{aligned} Z_n'(z) = & \lambda_n \cosh(\lambda_n z) - \frac{1}{H} \cosh(\lambda_n H) (\sinh(\lambda_n(z - H)) + \lambda_n z \cosh(\lambda_n(z - H))) \\ & + \frac{\cosh(\lambda_n H) - \lambda_n H \sinh(\lambda_n H)}{\lambda_n H^2} \cdot (\cosh(\lambda_n(z - H)) + \lambda_n z \sinh(\lambda_n(z - H))). \end{aligned} \quad (3.46)$$

This expression is much simpler after we put $z = 0$:

$$Z'_n(0) = \lambda_n + \frac{1}{H} \cosh(\lambda_n H) \sinh(\lambda_n H) + \frac{\cosh(\lambda_n H) - \lambda_n H \sinh(\lambda_n H)}{\lambda_n H^2} \cdot \cosh(\lambda_n H) \quad (3.47)$$

$$= \frac{\lambda_n^2 H^2 + \cosh^2(\lambda_n H)}{\lambda_n H^2}. \quad (3.48)$$

Finally we may substitute (3.48) into (3.45) and conclude that

$$\frac{\partial \psi_n}{\partial z}(x, 0) = [a_n \sin(\lambda_n x) + b_n \cos(\lambda_n x)]. \quad (3.49)$$

By taking $\Psi = \psi_0 + \sum_{n=1}^{\infty} \psi_n$ we obtain a streamfunction that satisfies (3.15).

3.4 Existence of Solutions for the Biharmonic Problem

We state our results in a compact form. Suppose that the basal sliding velocity in meters per second is given by

$$f = a_0 + \sum_{n=1}^{\infty} a_n \sin(\lambda_n x) + b_n \cos(\lambda_n x),$$

where $\lambda_n = \frac{2\pi n}{L}$ for each $n \in \mathbb{N}$. For each n define the functions

$$\begin{aligned} Z_n(z) &= \sinh(\lambda_n z) - \frac{1}{H} \cosh(\lambda_n H) z \sinh(\lambda_n(z - H)) \\ &+ \left(\frac{\cosh(\lambda_n H)}{\lambda_n H^2} - \frac{\sinh(\lambda_n H)}{H} \right) z \cosh(\lambda_n(z - H)) \end{aligned} \quad (3.50)$$

and

$$X_n(x) = \left(a_n \sin(\lambda_n x) + b_n \cos(\lambda_n x) \right) \frac{\lambda_n H^2}{\lambda_n^2 H^2 + \cosh^2(\lambda_n H)}. \quad (3.51)$$

Then the function

$$\Psi_2(x, z) = a_0 z + \sum_{n=1}^{\infty} X_n(x) Z_n(z) \quad (3.52)$$

is the unique solution of the boundary value problem (3.9)-(3.17) with the homogeneous version of (3.17). Finally

$$\begin{aligned}\Psi &= \Psi_1 + \Psi_2 \\ &= a_0 z + \frac{g_1 H}{2\mu} z^2 - \frac{g_1}{6\mu} z^3 + \sum_{n=1}^{\infty} X_n(x) Z_n(z)\end{aligned}$$

solves the original problem (3.9) - (3.17) with both nonhomogeneous boundary conditions. A classical uniqueness result for the biharmonic problem with Dirichlet and Neumann conditions imposed on the boundary appears on p.448 of [TS63]. We do not consider uniqueness with no-stress and periodic conditions.

3.5 Recovery of Velocity

We now differentiate the streamfunction Ψ to recover velocity. The horizontal velocity is

$$\begin{aligned}u(x, z) &= \Psi_z(x, z) \\ &= a_0 + \frac{g_1 H}{\mu} z - \frac{g_1}{2\mu} z^2 + \sum_{n=1}^{\infty} X_n(x) Z'_n(z)\end{aligned}\tag{3.53}$$

or, more explicitly,

$$u(x, z) = a_0 + \frac{g_1 H}{\mu} z - \frac{g_1}{2\mu} z^2 + \sum_{n=1}^{\infty} \frac{\lambda_n H^2}{\lambda_n^2 H^2 + \cosh^2(\lambda_n H)} (a_n \sin(\lambda_n x) + b_n \cos(\lambda_n x)) Z'_n(z)\tag{3.54}$$

where $Z'_n(z)$ is given by (3.46). For the vertical velocity we obtain

$$\begin{aligned}w(x, z) &= -\Psi_x(x, z) \\ &= 0 - \sum_{n=1}^{\infty} X'_n(x) Z_n(z)\end{aligned}\tag{3.55}$$

$$= \sum_{n=1}^{\infty} \frac{\lambda_n^2 H^2}{\lambda_n^2 H^2 + \cosh^2(\lambda_n H)} (b_n \sin(\lambda_n x) - a_n \cos(\lambda_n x)) Z_n(z).\tag{3.56}$$

3.6 Recovery of Pressure

Balise and Raymond did not give a formula for the pressure p in [BR85], being concerned only with the velocity. Recovering p takes more work than recovering \mathbf{u} since we need to go back to the Stokes equations, which contain only derivatives of p . Once we find the pressure gradient, we must antidifferentiate its two components and reconcile the constants of integration. This determines the pressure up to an additive constant and solves the Stokes problem in the form (3.2)-(3.8). However, we will see that the free surface condition in the original form $\sigma \cdot \mathbf{n} = 0$, unlike its relatives (3.7) and (3.8) stated in terms of \mathbf{u} , does determine the additive constant.

In the x -direction we have $p_x = \mu(u_{xx} + u_{zz}) + g_1$ and in the z -direction we have $p_z = \mu(w_{xx} + w_{zz}) + g_2$. We therefore begin by finding the second derivatives of the velocity components. Repeated differentiation of (3.53) and (3.55) gives the formulas

$$u_{xx} = \sum_{n=1}^{\infty} X_n'' Z_n' \quad (3.57)$$

$$u_{zz} = \frac{-g_1}{\mu} + \sum_{n=1}^{\infty} X_n Z_n''' \quad (3.58)$$

$$w_{xx} = - \sum_{n=1}^{\infty} X_n''' Z_n \quad (3.59)$$

$$w_{zz} = - \sum_{n=1}^{\infty} X_n' Z_n'' \quad (3.60)$$

Integrating in the z -direction, we obtain one expression for pressure:

$$p = \int p_z dz = \int \mu(w_{xx} + w_{zz}) + g_2 dz \quad (3.61)$$

$$= g_2 z + \mu \left[\sum_{n=1}^{\infty} -X_n''' \int Z_n dz + \sum_{n=1}^{\infty} -X_n' Z_n' \right] + C(x). \quad (3.62)$$

Here $C(x)$ represents a function which does not depend on z . Integrating in the x -direction,

we obtain another expression:

$$p = \int p_x dx = \int \mu(u_{xx} + u_{zz}) + g_1 dx \quad (3.63)$$

$$= g_1 x - \frac{g_1 \mu}{\mu} x + \mu \left[\sum_{n=1}^{\infty} X'_n Z'_n + \sum_{n=1}^{\infty} \left[\int X_n dx \right] Z_n''' \right] + C(z). \quad (3.64)$$

Note that the two linear terms in (3.64) cancel, so this is periodic in x as needed. To reconcile (3.62) and (3.64) we can let $C(x)$ be an arbitrary constant and take $C(z) = g_2 z + C(x)$; we then need only show that for each n we have

$$-X_n''' \int Z_n dz - X'_n Z'_n = X'_n Z'_n + \left[\int X_n dx \right] Z_n'''. \quad (3.65)$$

To verify this we recall that $X_n(x)$ is trigonometric, and so taking an even number of derivatives of $X_n(x)$ has the effect of multiplication by a power of $-\lambda_n^2$. We can therefore write X_n''' and $\int X_n dx$ in terms of $X'(x)$. The previous equation becomes

$$\lambda_n^2 X'_n \int Z_n dz - X'_n Z'_n = X'_n Z'_n - \frac{1}{\lambda_n^2} X'_n Z_n'''. \quad (3.66)$$

After rearrangement and multiplication by $-\lambda_n^2$ this gives

$$0 = X'_n \left(Z_n''' - 2\lambda_n^2 Z'_n + \lambda_n^4 \int Z_n \right). \quad (3.67)$$

It suffices to show that the factor involving Z_n vanishes. Recall that we constructed Z_n to solve the ODE (3.23). Hence the z -derivative of this factor vanishes. It follows that the factor itself vanishes for some choice of the constant of integration in (3.67). We conclude that the two expressions (3.62) and (3.64) are equal. It is unclear which is more convenient for computation; we take (3.64) which we restate, following some simplification and the substitution $C(x) = -g_2 H$:

$$p(x, z) = g_2 z - g_2 H + \mu \sum_{n=1}^{\infty} \frac{\lambda_n H^2 (a_n \cos(\lambda_n x) - b_n \sin(\lambda_n x))}{\lambda_n^2 H^2 + \cosh^2(\lambda_n H)} \left(\lambda_n Z'_n(z) - \frac{Z_n'''(z)}{\lambda_n} \right). \quad (3.68)$$

A simple formula for the factor in large parentheses is

$$\lambda_n Z_n'(z) - \frac{Z_n'''(z)}{\lambda_n} = \frac{2\lambda_n}{H} \sinh(\lambda_n z) - \frac{2 \cosh(H\lambda_n)}{H^2} \cosh(\lambda_n(z-H)). \quad (3.69)$$

This formula can be obtained from (3.46) and (3.29) using the formulas for c and d given in (3.35) and (3.36), by cancelling terms and then using the hyperbolic angle addition formula.

The value of the constant term $C(x)$ is irrelevant if we only want to solve the boundary value problem (3.2)-(3.8), since only derivatives of p appear. However, the boundary conditions (3.7)-(3.8) are weaker than the original stress-free condition $\boldsymbol{\sigma} \cdot \mathbf{n} = 0$, which does determine the constant term in p . We justify the choice $C(x) = -g_2 H$ in Section 3.8. For now we note that the choice $C(x) = -g_2 H$ gives zero pressure at the upper surface in the case of a no-slip condition at the base (i.e. if all a_n and b_n vanish).

We conclude this section by noting that the computability of equation (3.68) depends on the aspect ratio L/H and the number of Fourier terms used. Since $\lambda_n H = 2\pi n \frac{H}{L}$, the quantity $\cosh^2(\lambda_n H)$ appearing in the denominator of the pressure can cause overflow errors.

3.7 Stress at the Lower Boundary

Friction laws relating stress to velocity are more common than Dirichlet conditions at the base in numerical simulations. In this section we investigate what friction profile is necessary to generate a given basal velocity. We consider the linear law (2.38)-(2.39).

In the rectangular geometry considered before, we have $\mathbf{n} = (0, -1)$ and we take $\mathbf{t} = (1, 0)$. Then, with $\mathbf{u} = (u, w)$ as before, the impermeability condition (2.38) implies $w = 0$ and the stress relation (2.39) reduces to

$$-\sigma_{21} = -\beta^2 f \quad (3.70)$$

since $u|_{z=0} = f$. To find β^2 we need a formula for σ_{21} at the base. Under the linear flow law we have

$$\sigma_{21} = \tau_{21} = 2\mu \dot{\epsilon}_{21} = \mu \left(\frac{\partial w}{\partial x} + \frac{\partial u}{\partial z} \right) = \mu \frac{\partial u}{\partial z} \quad (3.71)$$

since $w \equiv 0$ on the base. We therefore differentiate (3.54) and (3.46) to find that

$$\frac{\partial u}{\partial z}(x, z) = \frac{g_1 H}{\mu} - \frac{g_1 z}{\mu} + \sum_{n=1}^{\infty} \frac{\lambda_n H^2}{\lambda_n^2 H^2 + \cosh^2(\lambda_n H)} (a_n \sin(\lambda_n x) + b_n \cos(\lambda_n x)) Z_n''(0) \quad (3.72)$$

where $Z_n''(z)$ is given by

$$\begin{aligned} Z_n''(z) &= \lambda_n^2 \sinh(\lambda_n z) - \frac{\lambda_n \cosh(\lambda_n H)}{H} (2 \cosh(\lambda_n(z - H)) + \lambda_n z \sinh(\lambda_n(z - H))) \\ &+ \frac{\cosh(\lambda_n H) - \lambda_n H \sinh(\lambda_n H)}{H^2} \cdot (2 \sinh(\lambda_n(z - H)) + \lambda_n z \cosh(\lambda_n(z - H))). \end{aligned} \quad (3.73)$$

Putting $z = 0$ we obtain

$$\begin{aligned} Z_n''(0) &= -\frac{2\lambda_n}{H} (\cosh^2(\lambda_n H) - \sinh^2(\lambda_n H)) - \frac{2 \cosh(\lambda_n H) \sinh(\lambda_n H)}{H^2} \\ &= -\frac{2\lambda_n H + \sinh(2\lambda_n H)}{H^2}. \end{aligned} \quad (3.74)$$

Hence a concise formula for σ_{21} along the lower boundary is

$$\sigma_{21}(x, 0) = g_1 H - \mu \sum_{n=1}^{\infty} \frac{2\lambda_n^2 H + \lambda_n \sinh(2\lambda_n H)}{\lambda_n^2 H^2 + \cosh^2(\lambda_n H)} (a_n \sin(\lambda_n x) + b_n \cos(\lambda_n x)). \quad (3.75)$$

Therefore an explicit expression for the basal friction coefficient β^2 as a function of the horizontal coordinate x is

$$\beta^2 = \frac{1}{f(x)} \left[g_1 H - \mu \sum_{n=1}^{\infty} \frac{2\lambda_n^2 H + \lambda_n \sinh(2\lambda_n H)}{\lambda_n^2 H^2 + \cosh^2(\lambda_n H)} (a_n \sin(\lambda_n x) + b_n \cos(\lambda_n x)) \right]. \quad (3.76)$$

It is interesting to note that the expression in brackets has average value 0 if $g_1 = 0$, which occurs if the slope angle is zero. In this case we can easily get a negative value for β^2 . On the other hand, any imposed basal velocity yields $\beta^2 > 0$ if it occurs under sufficiently large gravity. If we want $\beta^2 > 0$ we can no longer choose the basal velocity independently of the other parameters. We can state this as a theorem:

Theorem 3.7.1. *A basal velocity f with Fourier coefficients (a_n) and (b_n) can occur in a*

periodic Newtonian glacier of constant height H and slope angle α only if

$$\sin(\alpha)g\rho H > \mu \sum_{n=1}^{\infty} \frac{2\lambda_n^2 H + \lambda_n \sinh(2\lambda_n H)}{\lambda_n^2 H^2 + \cosh^2(\lambda_n H)} (a_n \sin(\lambda_n x) + b_n \cos(\lambda_n x)) \quad (3.77)$$

for all x .

3.8 Stress at the Upper Boundary

In this section we use the formulas for \mathbf{u} and p given above to obtain an explicit expression for the surface stress at $z = H$. This will allow us to justify the choice $C_x = -g_2 H$ for the constant term in the pressure formula (3.68) as well as to check our work by explicitly verifying that $\boldsymbol{\sigma} \cdot \mathbf{n} = 0$ at the free surface. The surface normal is $\mathbf{n} = (0, 1)$ and so we need expressions for the second column of $\boldsymbol{\sigma}$. We consider the two entries of this column separately.

For σ_{12} we can recycle some of the work of the last section. Instead of (3.71) we have

$$\sigma_{12} = \mu \left(\frac{\partial w}{\partial x} + \frac{\partial u}{\partial z} \right) \quad (3.78)$$

since $\frac{\partial w}{\partial x}$ does not vanish. To find $\frac{\partial w}{\partial x}$ we differentiate (3.56) with respect to x to obtain

$$\frac{\partial w}{\partial x}(x, z) = \sum_{n=1}^{\infty} \frac{\lambda_n^3 H^2}{\lambda_n^2 H^2 + \cosh^2(\lambda_n H)} (b_n \cos(\lambda_n x) + a_n \sin(\lambda_n x)) Z_n(z). \quad (3.79)$$

Putting $z = H$ in (3.50) gives

$$Z_n(H) = \frac{\cosh(\lambda_n H)}{\lambda_n H}, \quad (3.80)$$

so

$$\frac{\partial w}{\partial x}(x, H) = \sum_{n=1}^{\infty} \frac{\lambda_n^2 H \cosh(\lambda_n H)}{\lambda_n^2 H^2 + \cosh^2(\lambda_n H)} (b_n \cos(\lambda_n x) + a_n \sin(\lambda_n x)). \quad (3.81)$$

We now find $\frac{\partial u}{\partial z}$ at the upper surface by setting $z = H$ in (3.72). Putting $z = H$ in (3.73), we find after convenient cancellation that

$$Z_n''(H) = \frac{-\lambda_n}{H} \cosh(\lambda_n H) \quad (3.82)$$

and so

$$\frac{\partial u}{\partial z}(x, H) = - \sum_{n=1}^{\infty} \frac{\lambda_n^2 H \cosh(\lambda_n H)}{\lambda_n^2 H^2 + \cosh^2(\lambda_n H)} (a_n \sin(\lambda_n x) + b_n \cos(\lambda_n x)). \quad (3.83)$$

Now the sum of (3.81) and (3.83) is zero, so σ_{12} does indeed vanish at the upper surface.

For the other component of $\sigma \cdot \mathbf{n}$, we have

$$\sigma_{22} = -p + 2\mu \frac{\partial w}{\partial z}. \quad (3.84)$$

We therefore need expressions for pressure and $\frac{\partial w}{\partial z}$ along the upper surface. Putting $z = H$ in (3.68) (with constant term C_x) and (3.69) gives

$$\begin{aligned} p(x, H) &= g_2 H + C_x \\ &+ 2\mu \sum_{n=1}^{\infty} \frac{\lambda_n H (a_n \cos(\lambda_n x) - b_n \sin(\lambda_n x))}{\lambda_n^2 H^2 + \cosh^2(\lambda_n H)} \left(\lambda_n \sinh(\lambda_n H) - \frac{\cosh(\lambda_n H)}{H} \right). \end{aligned} \quad (3.85)$$

Differentiating (3.56) with respect to z gives

$$\frac{\partial w}{\partial z}(x, z) = \sum_{n=1}^{\infty} \frac{\lambda_n^2 H^2}{\lambda_n^2 H^2 + \cosh^2(\lambda_n H)} (b_n \sin(\lambda_n x) - a_n \cos(\lambda_n x)) Z'_n(z). \quad (3.86)$$

We gave a formula for $Z'_n(z)$ in (3.46). Putting $z = H$ gives

$$Z'_n(z) = \frac{\cosh(\lambda_n H) - \lambda_n H \sinh(\lambda_n H)}{\lambda_n H^2}. \quad (3.87)$$

Hence

$$\frac{\partial w}{\partial z}(x, H) = \sum_{n=1}^{\infty} \frac{\lambda_n (\cosh(\lambda_n H) - \lambda_n H \sinh(\lambda_n H))}{\lambda_n^2 H^2 + \cosh^2(\lambda_n H)} (b_n \sin(\lambda_n x) - a_n \cos(\lambda_n x)). \quad (3.88)$$

With these expressions for p and $\frac{\partial w}{\partial z}$, equation (3.84) becomes

$$\sigma_{22}(x, H) = -g_2 H - C_x. \quad (3.89)$$

To obtain $\sigma \cdot \mathbf{n} = 0$ it suffices to take $C_x = -g_2 H$. This justifies the choice of the constant

term in (3.68).

3.9 Qualitative Discussion

The formulas (3.54), (3.56), and (3.68) describe the components of velocity and pressure solving the Stokes problem (3.2)-(3.8). We note that the formulas are plausible in the sense that higher gravities and lower viscosities each result in faster flow.

For more detail it is helpful to consider a specific example. Consider a 40km long section of glacier of thickness 1km sitting on a bed of inclination 1.5° . We take $\rho = 917 \text{ kg m}^{-3}$, $g = 9.81 \text{ m sec}^{-2}$, and $\mu = 1 \times 10^{14} \text{ Pa sec}$. We specify a basal slip profile where most of the lower surface of the ice moves over the bedrock at a rate of 100 meters per year with the exception of one section which is almost frozen to the bed. To be specific, we take

$$f(x) = 200 \left[\frac{1}{1 + e^{120(x/L-0.3)}} + \frac{1}{1 + e^{120(-x/L+5)}} + 10^{-4} \right]. \quad (3.90)$$

Because f is smooth there is little harm in truncating its Fourier series; here we truncated the trigonometric expansion of f after the terms with λ_{50} . The resulting velocity field and pressure are illustrated in the central plot of Figure 3.2. As one would expect, there is a pressure maximum upstream of the obstacle and this maximum diminishes and spreads out with increasing height. If the melting and accumulation at the surface were such that the rectangular geometry were preserved over time, the ice particles would rise upstream of the obstacle or sticky spot and then fall back to their original depth downstream. For the given parameters and basal velocity we see a vertical velocity as high as 31.8 m/a at the surface above $x = 12 \text{ km}$, so the rectangular geometry would be unstable under any realistic surface accumulation regime.

The friction coefficient β^2 given by (3.76) is graphed in the lower plot of Figure 3.2. Its value is approximately $7.5 \times 10^{10} \text{ Pa s/m}$ away from the sticky spot; above the sticky spot it grows larger but remains finite since the basal velocity f is bounded away from zero.

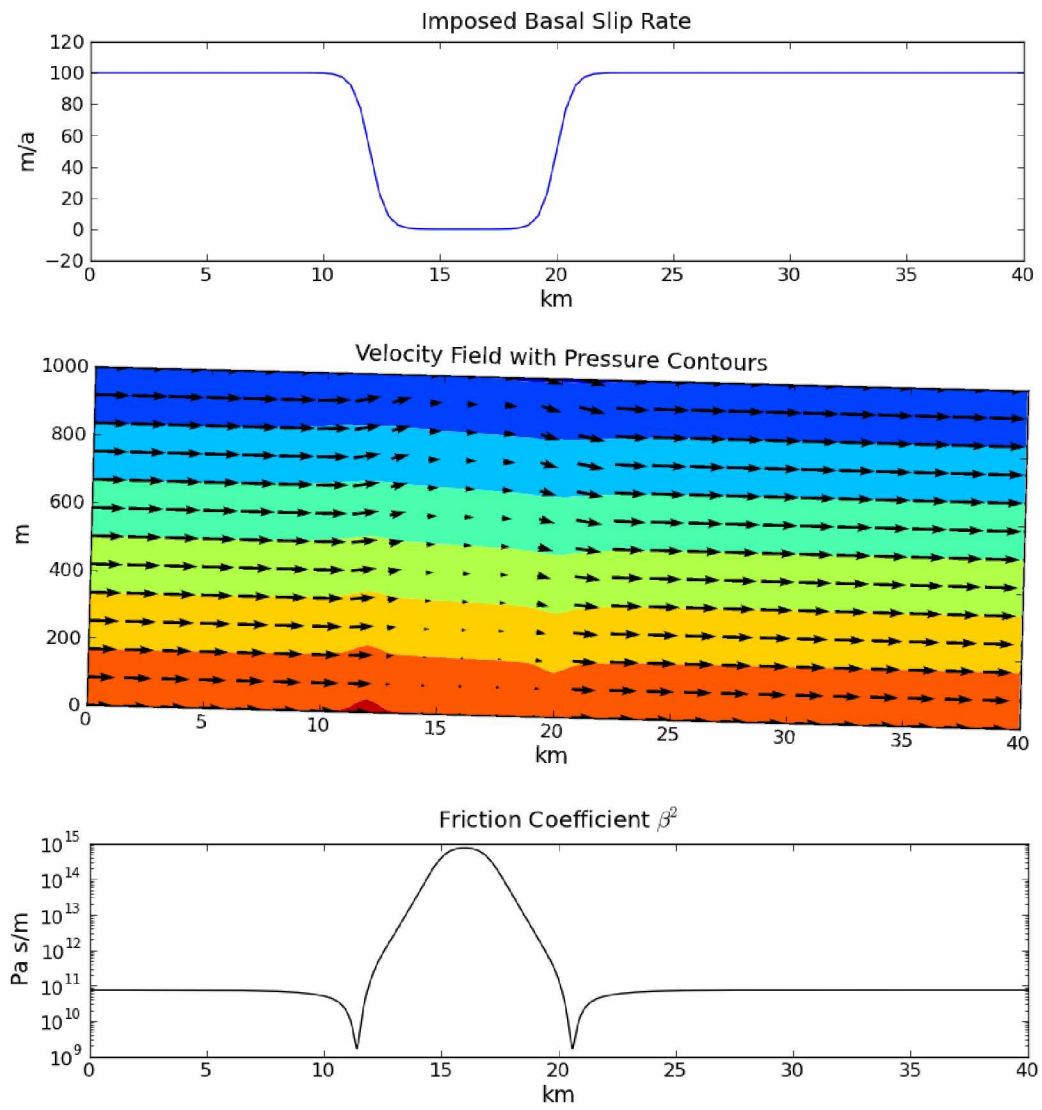


Figure 3.2. Exact velocity, pressure, and basal friction induced by a sticky spot.

Chapter 4

Finite Elements and the Stokes Problem

4.1 Introduction

In this chapter we develop a numerical technique for approximating the solutions of the Stokes boundary value problem considered in the previous chapter. This technique is an example of the widely used *finite element method* (FEM). For the Stokes flow problem, the common approach in introductory treatments of the FEM, e.g. [ESW05, QV94, Ern04, DH03] is to address only the simplest boundary conditions such as enclosed flow or flow through pipes with a Neumann condition at the exit. The bilinear form required to deal with the no-stress condition (2.37) appears in [Pir89, QV94] but these works do not state the Stokes equation in terms of the stress tensor or discuss the integration by parts. In contrast, the glaciological literature frequently employs (2.37) but omits the mathematical details of the finite element method: integration by parts, basis construction, matrix assembly, and solution of large linear systems. This chapter fills a pedagogical gap by discussing the Stokes problem at an introductory level while treating glaciologically-relevant boundary conditions. The presentation is based on a 2012 paper by Leng et al. [LJG⁺12] and the 2005 book by Elman et al., [ESW05]. We include many details omitted there; for example, Leng et al. skip from (4.1) to (4.12) in one sentence.

4.2 Variational Formulation

We begin by putting $\sigma = \tau - pI$ in the Stokes system (2.24) to obtain the system

$$\mathbf{0} = \nabla \cdot \tau - \nabla p + \rho \mathbf{g} \tag{4.1}$$

$$\mathbf{0} = \nabla \cdot \mathbf{u}. \tag{4.2}$$

We call this the *strong form* of the system in contrast to the *variational* or *weak formulation*, which we now derive.

Let \mathbf{u} and p be velocity and pressure fields satisfying the strong form of the Stokes system (we delay stating their relationship to τ). Let \mathbf{v} be any vector field whose components are all differentiable. Take a dot product with \mathbf{v} on each side of (4.1) and integrate over Ω to

obtain

$$-\int_{\Omega} (\nabla \cdot \tau) \cdot \mathbf{v} + \int_{\Omega} (\nabla p) \cdot \mathbf{v} = \rho \int_{\Omega} \mathbf{g} \cdot \mathbf{v}. \quad (4.3)$$

It is useful to rewrite this equation in a form containing boundary integrals. Our main tool for doing so is the Divergence Theorem $\int_{\Omega} \nabla \cdot \mathbf{f} = \int_{\partial\Omega} \mathbf{n} \cdot \mathbf{f}$. We therefore rewrite each integrand so that it contains a divergence. This procedure is called *integration by parts* because it ultimately depends on the product rule for derivatives.

For the pressure term in (4.3), we write

$$\int_{\Omega} (\nabla p) \cdot \mathbf{v} = \int_{\Omega} \frac{\partial p}{\partial x_i} v_i \quad (4.4)$$

$$= \int_{\Omega} \frac{\partial}{\partial x_i} (p v_i) - p \frac{\partial v_i}{\partial x_i} \quad (4.5)$$

$$= \int_{\Omega} \nabla \cdot (p \mathbf{v}) - p \nabla \cdot \mathbf{v} \quad (4.6)$$

$$= \int_{\partial\Omega} \mathbf{n} \cdot (p \mathbf{v}) - \int_{\Omega} p \nabla \cdot \mathbf{v}. \quad (4.7)$$

To deal with the stress term in (4.3) we make use of the symmetry of τ . Before integrating we have

$$\begin{aligned} -(\nabla \cdot \tau) \cdot \mathbf{v} &= -\frac{\partial \tau_{ij}}{\partial x_j} v_i \\ &= \tau_{ij} \frac{\partial v_i}{\partial x_j} - \frac{\partial}{\partial x_j} (\tau_{ij} v_i) \\ &= \tau_{ji} \frac{\partial v_i}{\partial x_j} - \nabla \cdot (\tau \cdot \mathbf{v}) \\ &= \tau_{ji} (\nabla \mathbf{v})_{ji} - \nabla \cdot (\tau \cdot \mathbf{v}) \\ &= \tau : \nabla \mathbf{v} - \nabla \cdot (\tau \cdot \mathbf{v}). \end{aligned} \quad (4.8)$$

Here $\tau \cdot \mathbf{v}$ is the usual matrix-vector product, and $\tau : \nabla \mathbf{v} = \tau_{ij} (\nabla \mathbf{v})_{ij}$ denotes the sum of the components of the elementwise product of these tensors. Integration now gives

$$-\int_{\Omega} (\nabla \cdot \tau) \cdot \mathbf{v} = \int_{\Omega} \tau : \nabla \mathbf{v} - \int_{\partial\Omega} \mathbf{n} \cdot (\tau \cdot \mathbf{v}). \quad (4.9)$$

Adding equations (4.7) and (4.9), we obtain

$$\begin{aligned}
-\int_{\Omega} (\nabla \cdot \tau) \cdot \mathbf{v} + \int_{\Omega} (\nabla p) \cdot \mathbf{v} &= \int_{\Omega} \tau : \nabla \mathbf{v} - \int_{\Omega} p \nabla \cdot \mathbf{v} + \int_{\partial\Omega} \mathbf{n} \cdot (p\mathbf{v}) - \int_{\partial\Omega} \mathbf{n} \cdot (\tau \cdot \mathbf{v}) \\
&= \int_{\Omega} \tau : \nabla \mathbf{v} - \int_{\Omega} p \nabla \cdot \mathbf{v} - \int_{\partial\Omega} \mathbf{n} \cdot (-p\mathbf{v} + \tau \cdot \mathbf{v}) \\
&= \int_{\Omega} \tau : \nabla \mathbf{v} - \int_{\Omega} p \nabla \cdot \mathbf{v} - \int_{\partial\Omega} \mathbf{n} \cdot (\sigma \cdot \mathbf{v}). \tag{4.10}
\end{aligned}$$

Note that the Cauchy stress tensor $\sigma = -pI + \tau$ has appeared in the boundary term in the last line. This will become important when we consider the boundary conditions. For now we observe that the parentheses are not important since, by the symmetry of σ ,

$$\mathbf{n} \cdot (\sigma \cdot \mathbf{v}) = n_i \sigma_{ij} v_j = n_i \sigma_{ji} v_j = (\mathbf{n} \cdot \sigma) \cdot \mathbf{v}. \tag{4.11}$$

We have shown that (4.3) implies

$$\int_{\Omega} \tau : \nabla \mathbf{v} - \int_{\Omega} p \nabla \cdot \mathbf{v} - \int_{\partial\Omega} \mathbf{n} \cdot \sigma \cdot \mathbf{v} = \rho \int_{\Omega} \mathbf{g} \cdot \mathbf{v}. \tag{4.12}$$

We now proceed to suppress the τ and σ appearing in (4.12) in favor of \mathbf{u} , \mathbf{v} , and p . To write $\tau : \nabla \mathbf{v}$ in terms of \mathbf{u} and \mathbf{v} we first exploit the symmetry of τ :

$$\begin{aligned}
\tau_{ij}(\nabla \mathbf{v})_{ij} &= \tau_{ij} \frac{\partial v_j}{\partial x_i} \\
&= \frac{1}{2} (\tau_{ij} + \tau_{ji}) \frac{\partial v_j}{\partial x_i} \\
&= \frac{1}{2} \tau_{ij} \frac{\partial v_j}{\partial x_i} + \frac{1}{2} \tau_{ji} \frac{\partial v_j}{\partial x_i} \\
&= \frac{1}{2} \tau_{ij} \frac{\partial v_j}{\partial x_i} + \frac{1}{2} \tau_{ij} \frac{\partial v_i}{\partial x_j} \\
&= \frac{1}{2} \tau_{ij} \left(\frac{\partial v_j}{\partial x_i} + \frac{\partial v_i}{\partial x_j} \right). \tag{4.13}
\end{aligned}$$

Now we use the linear viscosity assumption $\tau = 2\mu\dot{\epsilon}$. This gives

$$\begin{aligned}
\tau_{ij}(\nabla \mathbf{v})_{ij} &= \frac{1}{2} \cdot 2\mu \dot{\epsilon}_{ij} (\nabla \mathbf{v} + \nabla \mathbf{v}^T)_{ij} \\
&= \frac{1}{2} \mu (\nabla \mathbf{u}^T + \nabla \mathbf{u})_{ij} (\nabla \mathbf{v} + \nabla \mathbf{v}^T)_{ij}. \tag{4.14}
\end{aligned}$$

To address the boundary integral in (4.12) we consider the boundary subdomains separately. We write $\partial\Omega = \Gamma_b \cup \Gamma_s \cup \Gamma_r \cup \Gamma_l$, with the subscripts signifying the glacier bed, surface, and right and left boundaries respectively. On Γ_s , the stress-free boundary condition (2.37), i.e. $\boldsymbol{\sigma} \cdot \mathbf{n} = 0$, gives

$$-\int_{\Gamma_s} \mathbf{n} \cdot \boldsymbol{\sigma} \cdot \mathbf{v} = -\int_{\Gamma_s} \mathbf{0} \cdot \mathbf{v} = 0. \quad (4.15)$$

At the base we ensure that $-\int_{\Gamma_b} \mathbf{n} \cdot \boldsymbol{\sigma} \cdot \mathbf{v}$ vanishes by requiring that $\mathbf{v}|_{\Gamma_b} = \mathbf{0}$. Because the normal vector on Γ_l is the opposite of the normal on Γ_r , the integrals over the lateral boundaries will cancel each other if \mathbf{v} and $\boldsymbol{\sigma}$ are periodic. We therefore investigate what periodicity requirements on \mathbf{u} and p are necessary to ensure that $(\boldsymbol{\sigma} \cdot \mathbf{n})|_{\Gamma_l} = -(\boldsymbol{\sigma} \cdot \mathbf{n})|_{\Gamma_r}$. Because $\mathbf{n} = \pm(1, 0)$ we have

$$\boldsymbol{\sigma} \cdot \mathbf{n} = \pm \begin{bmatrix} 2\frac{\partial u_1}{\partial x_1} - p \\ \frac{\partial u_1}{\partial x_2} + \frac{\partial u_2}{\partial x_1} \end{bmatrix}. \quad (4.16)$$

It therefore suffices to require periodicity in $\frac{\partial u_1}{\partial x_1}$, in the sum $\frac{\partial u_1}{\partial x_2} + \frac{\partial u_2}{\partial x_1}$, and in p . This is similar to the boundary condition (3.5) in that it enforces two periodic constraints on the partial derivatives of \mathbf{u} .

We can now state the variational form of the problem. Define the function spaces

$$\mathbf{H}_E^1 = \left\{ \mathbf{u} \in H^1(\Omega)^2 : \mathbf{u}|_{\Gamma_b} = \mathbf{w}, \left(\mathbf{u}, \frac{\partial u_1}{\partial x_1}, \frac{\partial u_1}{\partial x_2} + \frac{\partial u_2}{\partial x_1} \right) \Big|_{\Gamma_l} = \left(\mathbf{u}, \frac{\partial u_1}{\partial x_1}, \frac{\partial u_1}{\partial x_2} + \frac{\partial u_2}{\partial x_1} \right) \Big|_{\Gamma_r} \right\} \quad (4.17)$$

$$\mathbf{H}_{E_0}^1 = \{ \mathbf{v} \in H^1(\Omega)^2 : \mathbf{v}|_{\Gamma_r} = \mathbf{v}|_{\Gamma_l}, \mathbf{v}|_{\Gamma_b} = \mathbf{0} \} \quad (4.18)$$

$$P_E = \{ p \in L^2(\Omega) : p|_{\Gamma_r} = p|_{\Gamma_l} \}. \quad (4.19)$$

We say that the pair $(\mathbf{u}, p) \in \mathbf{H}_E^1 \times P_E$ is a *weak solution* and that (\mathbf{u}, p) *solves the variational problem* if for all $(\mathbf{v}, q) \in \mathbf{H}_{E_0}^1 \times L^2(\Omega)$ we have

$$\frac{1}{2}\mu \int_{\Omega} (\nabla \mathbf{u}^T + \nabla \mathbf{u}) : (\nabla \mathbf{v} + \nabla \mathbf{v}^T) - \int_{\Omega} p \nabla \cdot \mathbf{v} = \rho \int_{\Omega} \mathbf{g} \cdot \mathbf{v}, \quad (4.20)$$

$$\int_{\Omega} q \nabla \cdot \mathbf{u} = 0. \quad (4.21)$$

This pair of equations is, perhaps surprisingly, equivalent to their sum

$$\frac{1}{2}\mu \int_{\Omega} (\nabla \mathbf{u}^T + \nabla \mathbf{u}) : (\nabla \mathbf{v} + \nabla \mathbf{v}^T) - \int_{\Omega} p \nabla \cdot \mathbf{v} + \int_{\Omega} q \nabla \cdot \mathbf{u} = \rho \int_{\Omega} \mathbf{g} \cdot \mathbf{v}. \quad (4.22)$$

To see this, note that if (4.22) holds for all $(\mathbf{v}, q) \in H_{E_0}^1 \times L^2(\Omega)$, then it holds for all $(\mathbf{v}, 0)$ which implies (4.20). Similarly we can take $\mathbf{v} = 0$ in (4.22) to obtain (4.21).

In the variational form of the problem we are requiring only that $(\mathbf{u}, p) \in \mathbf{H}_E^1 \times P_E$, so the velocity has square-integrable first derivatives and the pressure is merely square integrable. These are much weaker requirements than in the strong form (2.26), where \mathbf{u} needs second derivatives and p needs first derivatives. This difference is the origin of the terminology *strong* and *weak* for these problems and their solutions. A strong solution, if we can find it, will also be a weak solution, but the converse is not obviously true.

4.3 Discretisation

The weak formulation derived above is still a continuous problem stated in terms of infinite-dimensional vector spaces¹. The exact solution may not be available. However, we can approximate the weak form by a discrete problem stated in terms of a finite-dimensional vector space. The idea of the finite element method is to reduce the number of constraints: we will accept a pair (\mathbf{u}, p) as an approximate solution if it satisfies (4.22) for each (\mathbf{v}, q) in a *finite*-dimensional subspace of $\mathbf{H}_{E_0}^1 \times L^2(\Omega)$. We will prove that there exists a unique such pair in a finite-dimensional space approximating $\mathbf{H}_E^1 \times P_E$. We begin with the description of these finite-dimensional subspaces and the construction of useful bases for them. Once that is accomplished, we show how to construct a system of linear equations whose solution determines \mathbf{u} and p .

4.3.1 Some finite dimensional function spaces

Consider a triangular mesh with n nodes on Ω , that is, a triangulation of Ω such that the union of the interiors of the edges is disjoint from the set of nodes (vertices). Let M denote the subspace of $L^2(\Omega)$ consisting of continuous functions which are linear in the interior of

¹It is customary to note that \mathbf{H}_E^1 is a vector space only when $\mathbf{w} \equiv \mathbf{0}$. For other \mathbf{w} it is an affine translation of the $\mathbf{w} \equiv \mathbf{0}$ case. By a *subspace* of such a translate we mean a suitable translate of a subspace of the $\mathbf{w} \equiv \mathbf{0}$ space.

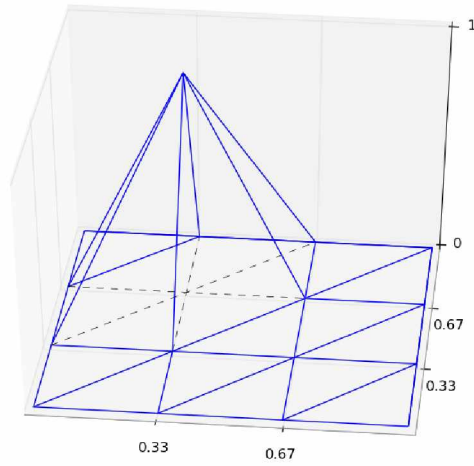


Figure 4.1. A pressure basis function $\psi_i \in M$ graphed on the edges of a triangular mesh.

each triangle. A function $q \in M$ is determined within each triangle by its values on the three vertices of the triangle, and hence q is uniquely determined by its values on the n nodes. This indicates that M is an n -dimensional vector space. We specify the convenient basis $\{\psi_0, \dots, \psi_{n-1}\}$ where ψ_i is the unique function in M taking the value 1 at the i -th node and 0 at all other nodes. A typical ψ_i is depicted in Figure 4.1.

For the velocity we use a richer function space, for reasons that will become clear later. We begin by defining the scalar function space to which the velocity components will belong. Using the same triangular mesh, let X denote the set of continuous functions which are biquadratic in the interior of each triangle, i.e, the continuous functions whose restrictions to any triangle have the form

$$c_1x^2 + c_2z^2 + c_3xz + c_4x + c_5z + c_6$$

for some constants c_i . There are six constants, so a function in X is uniquely determined within each triangle by its value at six distinct points on that triangle. We choose to specify functions in X by giving their values on the midpoints of each edge and on the vertices. This scheme gives the required six points on each triangle and also ensures continuity across edges, since quadratic functions on a segment coincide if they agree at three points.

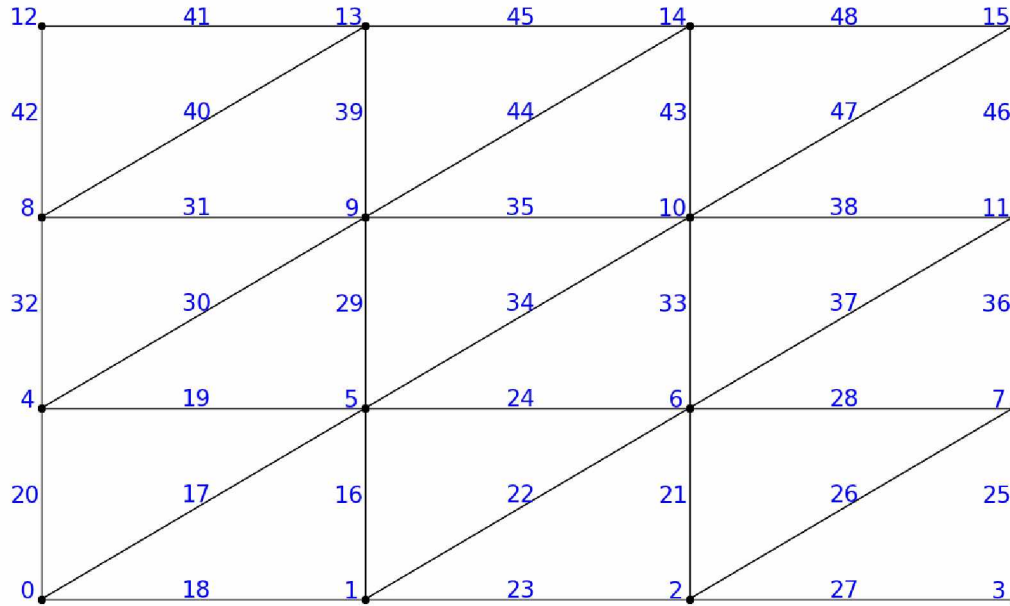


Figure 4.2. An ordering of vertices and edge midpoints with $n = 16$ and $r = 49$.

To construct an explicit basis, let r denote the number of vertices and edges in the mesh and let $\{P_0, P_1, \dots, P_{r-1}\}$ be some ordering of the vertices and edge midpoints. As a practical example of such an ordering consider Figure 4.2; this ordering is employed in the finite element software FEniCS.

We then define the basis $\{\phi_i\}_{i=0}^{r-1}$ by requiring $\phi_i(P_j) = \delta_{ij}$. If P_i is a point, this implies that ϕ_i vanishes on any triangle without P_i as a vertex; if P_i is an edge midpoint, then ϕ_i vanishes on any triangle whose boundary does not contain that edge. We graph two of these functions (ϕ_{13} and ϕ_{45} according to the ordering of Figure 4.2) in Figure 4.3.

Now define a space of vector functions $\mathbf{X} = X \times X$ to represent velocity fields. We choose

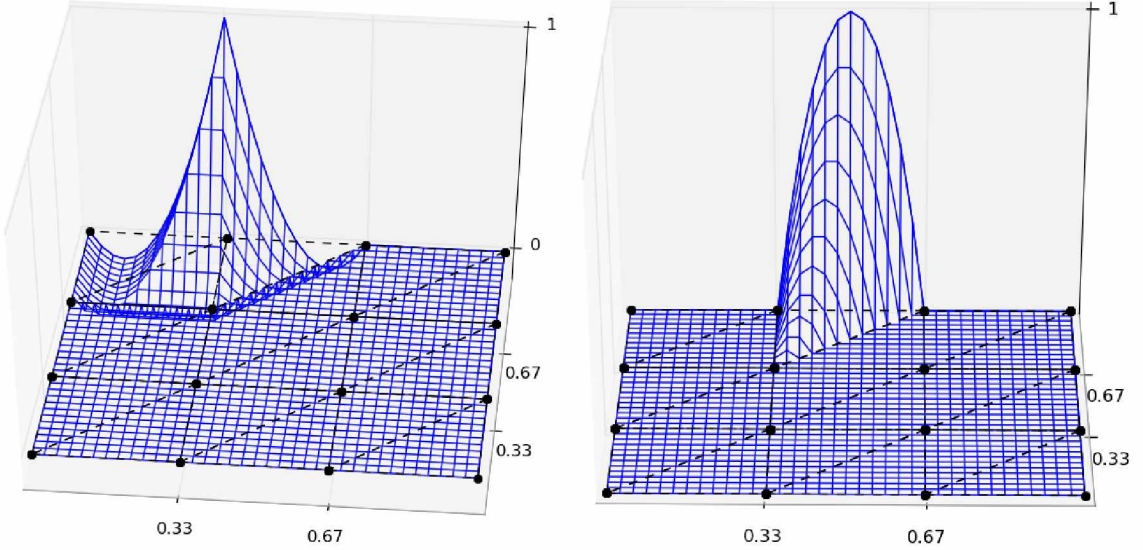


Figure 4.3. Velocity component basis functions $\phi_{13}, \phi_{45} \in X$.

a basis $\{\phi_i\}_{i=0}^{2(r)-1}$ by treating the two coordinates in sequence. Specifically, we define:

$$\phi_0 = (\phi_0, 0), \quad (4.23)$$

...

$$\phi_{r-1} = (\phi_{r-1}, 0), \quad (4.24)$$

$$\phi_r = (0, \phi_0), \quad (4.25)$$

...

$$\phi_{2r-1} = (0, \phi_{r-1}). \quad (4.26)$$

The scalar basis functions ϕ_i have the convenient property that ϕ_i vanishes at each P_j such that $i \neq j$. For the vector basis functions the corresponding condition is given by interpreting the point index modulo r . That is, ϕ_i vanishes at each P_j such that $i \equiv j \pmod{r}$. We therefore assume that all point indices are interpreted modulo r .

We now have a basis for the finite-dimensional subspaces $\mathbf{X} \subset \mathbf{H}^1(\Omega)$ and $M \subset L^2(\Omega)$. The space \mathbf{X} will contain both the approximate solution \mathbf{u} and the test functions \mathbf{v} . Recall that on the Dirichlet boundary Γ_b our test functions must vanish and the approximate velocity must interpolate \mathbf{w} , and both \mathbf{u} and \mathbf{v} should be periodic. Therefore we define two

subspaces of \mathbf{X} :

$$\mathbf{X}_0 = \{\mathbf{v} \in \mathbf{X} : \mathbf{v}|_{P_i} = 0 \text{ for all } P_i \in \Gamma_b, \mathbf{v}|_{\Gamma_l} = \mathbf{v}|_{\Gamma_r}\} \quad (4.27)$$

$$\mathbf{X}_w = \{\mathbf{u} \in \mathbf{X} : \mathbf{u}|_{P_i} = \mathbf{w}|_{P_i} \text{ for all } P_i \in \Gamma_b, \mathbf{u}|_{\Gamma_l} = \mathbf{u}|_{\Gamma_r}\}. \quad (4.28)$$

The *discrete form* of the problem is to find $(\mathbf{u}, p) \in \mathbf{X}_w \times M$ such that (4.22) holds for all $(\mathbf{v}, q) \in \mathbf{X}_0 \times M$. Note that we have discarded the periodicity requirements on the derivatives of \mathbf{u} in the discrete problem.

We are now ready to set up the linear system mentioned previously.

4.3.2 A linear algebra problem

If (\mathbf{u}, p) solves the discrete problem, then we can find coefficient vectors $\hat{\mathbf{u}} \in \mathbb{R}^{2r}$ and $\hat{\mathbf{p}} \in \mathbb{R}^n$ expanding them in the bases for \mathbf{X} and M above:

$$\mathbf{u} = \sum_{j=0}^{2r-1} \hat{u}_j \phi_j \quad (4.29)$$

$$p = \sum_{j=0}^{n-1} \hat{p}_j \psi_j. \quad (4.30)$$

The problem is to determine $\hat{\mathbf{u}}$ and $\hat{\mathbf{p}}$. Some entries of $\hat{\mathbf{u}}$ are determined immediately by the Dirichlet condition at the base. We interpolate \mathbf{w} by setting

$$(\hat{u}_i, \hat{u}_{i+r}) = \mathbf{w}|_{P_i} \quad (4.31)$$

for each $i < r$ such that $P_i \in \Gamma_b$.

To determine $\hat{\mathbf{p}}$ and the remaining entries of $\hat{\mathbf{u}}$, we suppose that (4.20) holds for each $\mathbf{v} \in \mathbf{X}_0$ and that (4.21) holds for each $q \in M$. For simplicity and to mimic the procedure used by FEniCS, we will ignore the periodicity requirements of these spaces while first assembling the system and account for them later by modifying that system. Therefore we assume for now that a basis for \mathbf{X}_0 is the set of ϕ_i such that $P_i \notin \Gamma_b$. For each such i we

take $\mathbf{v} = \boldsymbol{\phi}_i$ in (4.20) to find that

$$\frac{\mu}{2} \int_{\Omega} (\nabla \mathbf{u} + \nabla \mathbf{u}^T) : (\nabla \boldsymbol{\phi}_i + \nabla \boldsymbol{\phi}_i^T) - \int_{\Omega} p \nabla \cdot \boldsymbol{\phi}_i = \rho \int_{\Omega} \mathbf{g} \cdot \boldsymbol{\phi}_i. \quad (4.32)$$

Using the linearity of the inner product and the derivative, integral, and transpose operators, we now rewrite the first term of (4.32). We abandon the Einstein convention since we need explicit control over the values taken by the indices i and j in the sum. We have

$$\frac{\mu}{2} \int_{\Omega} \left(\nabla \sum_{j=0}^{2r-1} \hat{u}_j \boldsymbol{\phi}_j + \nabla \left(\sum_{j=0}^{2r-1} \hat{u}_j \boldsymbol{\phi}_j \right)^T \right) : (\nabla \boldsymbol{\phi}_i + \nabla \boldsymbol{\phi}_i^T) \quad (4.33)$$

$$= \sum_{j=0}^{2r-1} \hat{u}_j \left(\frac{\mu}{2} \int_{\Omega} (\nabla \boldsymbol{\phi}_j + \nabla \boldsymbol{\phi}_j^T) : (\nabla \boldsymbol{\phi}_i + \nabla \boldsymbol{\phi}_i^T) \right) \quad (4.34)$$

$$= \sum_{j: P_j \notin \Gamma_b} A_{ij} \hat{u}_j + \sum_{j: P_j \in \Gamma_b} A_{ij} \hat{u}_j \quad (4.35)$$

where the entries of $A \in \mathbb{R}^{2r \times 2r}$ are defined by taking A_{ij} equal to the factor multiplying \hat{u}_j in (4.34). We can rewrite the pressure term in (4.32) by expanding p :

$$- \int_{\Omega} \left(\sum_{j=0}^{n-1} \hat{p}_j \psi_j \right) \nabla \cdot \boldsymbol{\phi}_i = \sum_{j=0}^{n-1} p_j \left(- \int_{\Omega} \psi_j \nabla \cdot \boldsymbol{\phi}_i \right) = \sum_{j=0}^{n-1} B_{ij} p_j \quad (4.36)$$

where $B \in \mathbb{R}^{2r \times n}$ is defined by $B_{ij} = - \int_{\Omega} \psi_j \nabla \cdot \boldsymbol{\phi}_i$. Hence for each i such that $P_i \notin \Gamma_D$, the following restatement of (4.32) holds:

$$\sum_{j: P_j \notin \Gamma_b} A_{ij} \hat{u}_j + \sum_{j=0}^{n-1} B_{ij} p_j = - \sum_{j: P_j \in \Gamma_b} A_{ij} \hat{u}_j + \rho \int_{\Omega} \mathbf{g} \cdot \boldsymbol{\phi}_i \quad (4.37)$$

Similarly, for each $0 \leq i < n$ we take $q = \psi_i$ in (4.21) to obtain

$$0 = \int_{\Omega} \psi_i \nabla \cdot \mathbf{u} = \int_{\Omega} \psi_i \nabla \cdot \left(\sum_{j=0}^{2r-1} \hat{u}_j \boldsymbol{\phi}_j \right) = \sum_{j=0}^{2r-1} \hat{u}_j \int_{\Omega} \psi_i \nabla \cdot \boldsymbol{\phi}_j = \sum_{j=0}^{2r-1} B_{ji} \hat{u}_j \quad (4.38)$$

or

$$\sum_{j:P_j \notin \Gamma_b} B_{ji} \hat{u}_j = - \sum_{j:P_j \in \Gamma_b} B_{ji} \hat{u}_j. \quad (4.39)$$

Equations (4.37) and (4.39) constitute a linear system where the unknowns are $\hat{\mathbf{p}}$ and those entries $\tilde{\mathbf{u}}$ of $\hat{\mathbf{u}}$ that are not determined by the Dirichlet boundary condition. This system has the block matrix form

$$\begin{bmatrix} \tilde{A} & \tilde{B} \\ \tilde{B}^T & 0 \end{bmatrix} \begin{bmatrix} \tilde{\mathbf{u}} \\ \hat{\mathbf{p}} \end{bmatrix} = \begin{bmatrix} \mathbf{f} \\ \mathbf{g} \end{bmatrix}. \quad (4.40)$$

where \tilde{A} is formed from A by dropping the i -th row and column whenever $P_i \in \Gamma_D$, \tilde{B} is formed from B by dropping the i -th row whenever $P_i \in \Gamma_D$, and \mathbf{f} and \mathbf{g} are given by

$$f_i = - \sum_{j:P_j \in \Gamma_D} A_{ij} \hat{u}_j + \rho \int_{\Omega} \mathbf{g} \cdot \boldsymbol{\phi}_i \quad (4.41)$$

$$g_k = - \sum_{j:P_j \in \Gamma_D} \hat{u}_j \int_{\Omega} \psi_k \nabla \cdot \boldsymbol{\phi}_j. \quad (4.42)$$

We can combine (4.40) and (4.31) into a single larger linear system by interpreting (4.31) as a diagonal system. Instead of adding (4.31) as a single diagonal block, we intersperse these new equations in order to replace the rows and columns that were discarded in forming \tilde{A} and \tilde{B} from A and B . The sparsity structure of this system is illustrated in Figure 4.4 in the case of the mesh and numbering of Figure 4.2. This structure deserves a bit of attention, if only as a review of the ideas of this section. We will make several observations about Figure 4.4 and then seek to explain them.

- Rows 0, 1, 2, 3, 18, 23, and 27 have nonzero entries only on the diagonal. These are the numbers appearing on the lower boundary in Figure 4.2 and this corresponds to imposing a Dirichlet condition on the horizontal component of velocity at the base. The indices of the other rows with this property can be obtained by adding 49 to each of these numbers (thus 49, 50, 51, 52, 67, 72, 76), corresponding to the imposition of vertical velocity 0 at the base. These diagonal entries are not all ones in this implementation; after storing the system as \mathbf{A} we can see them at the command line:

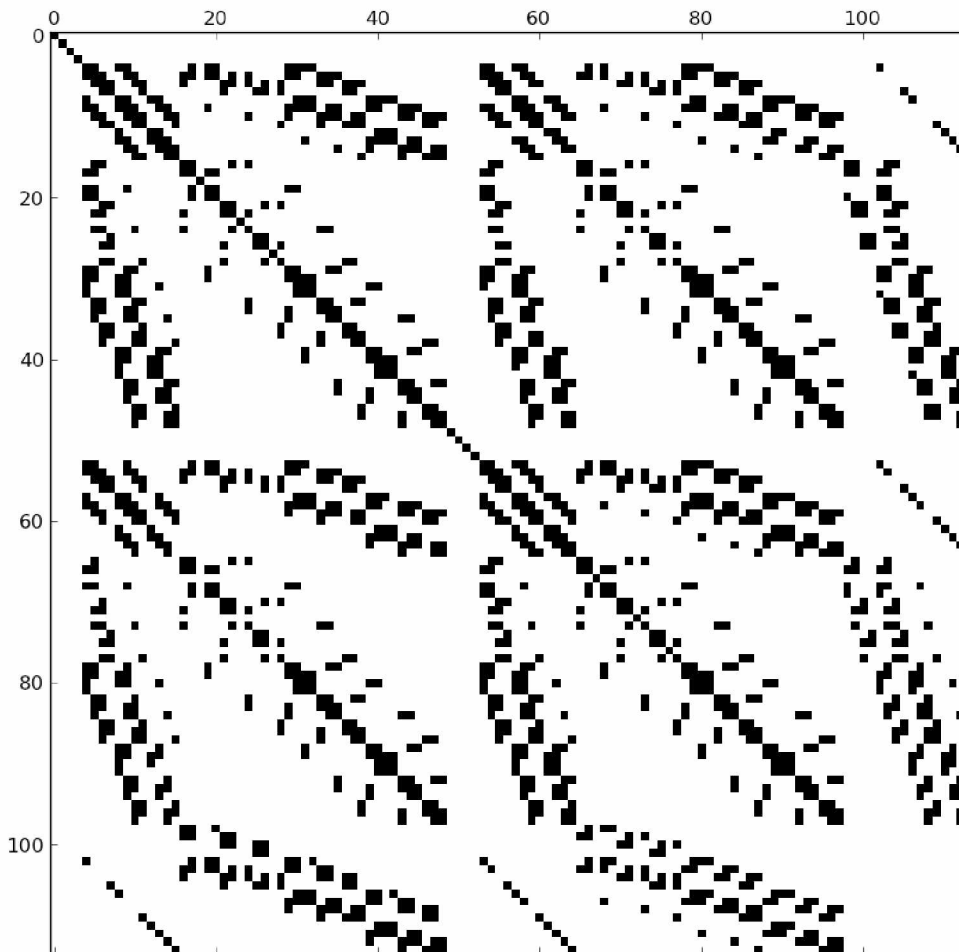


Figure 4.4. Sparsity structure of (4.40) augmented by Dirichlet conditions.

```
In [95]: DirichletDs = array([0,18,1,23,2,27,3,49,67,50,72,51,76,52])
In [96]: (diag(A)[DirichletDs]).reshape((2,7))
Out[96]:
array([[ 2.,  1.,  3.,  1.,  3.,  1.,  1.],
       [ 2.,  1.,  3.,  1.,  3.,  1.,  1.]])
```

The numbers in `DirichletDs` can be read in order along the lower boundary in Figure 4.2 from left to right. The corresponding diagonal entries coincide with the numbers of mesh cells adjacent to the nodes (e.g. P_2 is adjacent to three cells and $A_{22} = 3$).

We cannot explain this structure without a deeper investigation into FEniCS's matrix assembly methods.

- The lower diagonal block of zeros is small: $n \times n = 16 \times 16$. This is a consequence of our choice of a richer space for the velocity approximation than for the pressure. There are 16 degrees of freedom in choosing p but $2[49 - 7] = 84$ for \mathbf{u} if we do not count those used to interpolate \mathbf{w} on the base. The system is singular if the zero block is too large, so the importance of a rich velocity space should now be apparent.
- The system has block structure on a medium scale and on a fine scale, beyond the large scale indicated in equation (4.40). The medium level, consisting of four apparent 49×49 blocks, reflects the organization of equations (4.23)-(4.26) defining our construction of the vectors $\boldsymbol{\phi}_i$ from the scalar functions ϕ_i . Within these medium blocks we can discern still more structure, i.e. diagonal sub-blocks of dimension 16 and 33 respectively. This fine structure comes from our choosing to enumerate the vertices before the edges in 4.2. The numbering of the evaluation points determines the sparsity structure of A . For example, $A_{0,10} = \frac{\mu}{2} \int_{\Omega} (\nabla \phi_{10} + \nabla \phi_{10}^T) : (\nabla \psi_0 + \nabla \psi_0^T)$ will vanish because we see in Figure 4.2 that no triangle contains both nodes 0 and 10. Consequently the supports of ϕ_0 and ϕ_{18} do not meet, and so neither do those of $\boldsymbol{\phi}_0$ and $\boldsymbol{\phi}_{18}$.

We now alter our system of linear equations to enforce the periodic boundary conditions. The periodic condition is equivalent to glueing the lateral sides of the rectangle to form a cylinder, whereupon we find fewer nodes and different basis functions. If i_1 and i_2 are indices for degrees of freedom which are to be glued (e.g. 4 and 7 or 49 and 50 using the order in Figure 4.2), then we may no longer put $\mathbf{v} = \boldsymbol{\phi}_{i_1}$ or $\mathbf{v} = \boldsymbol{\psi}_{i_2}$ in (4.20). These two equations are lost from our system. On the other hand, we can take $\mathbf{v} = \boldsymbol{\phi}_{i_1} + \boldsymbol{\phi}_{i_2}$ in (4.20) as this is a periodic function; this gives an equation similar to (4.37):

$$\sum_{j:P_j \notin \Gamma_D} (A_{i_1j} + A_{i_2j}) \hat{u}_j + \sum_{j=0}^{n-1} (B_{i_1j} + B_{i_2j}) p_j = - \sum_{j:P_j \in \Gamma_D} (A_{i_1j} + A_{i_2j}) \hat{u}_j + \rho \int_{\Omega} \mathbf{g} \cdot (\boldsymbol{\phi}_{i_1} + \boldsymbol{\phi}_{i_2}). \quad (4.43)$$

Indeed, this equation is the sum of the two equations we threw out. This leaves one fewer

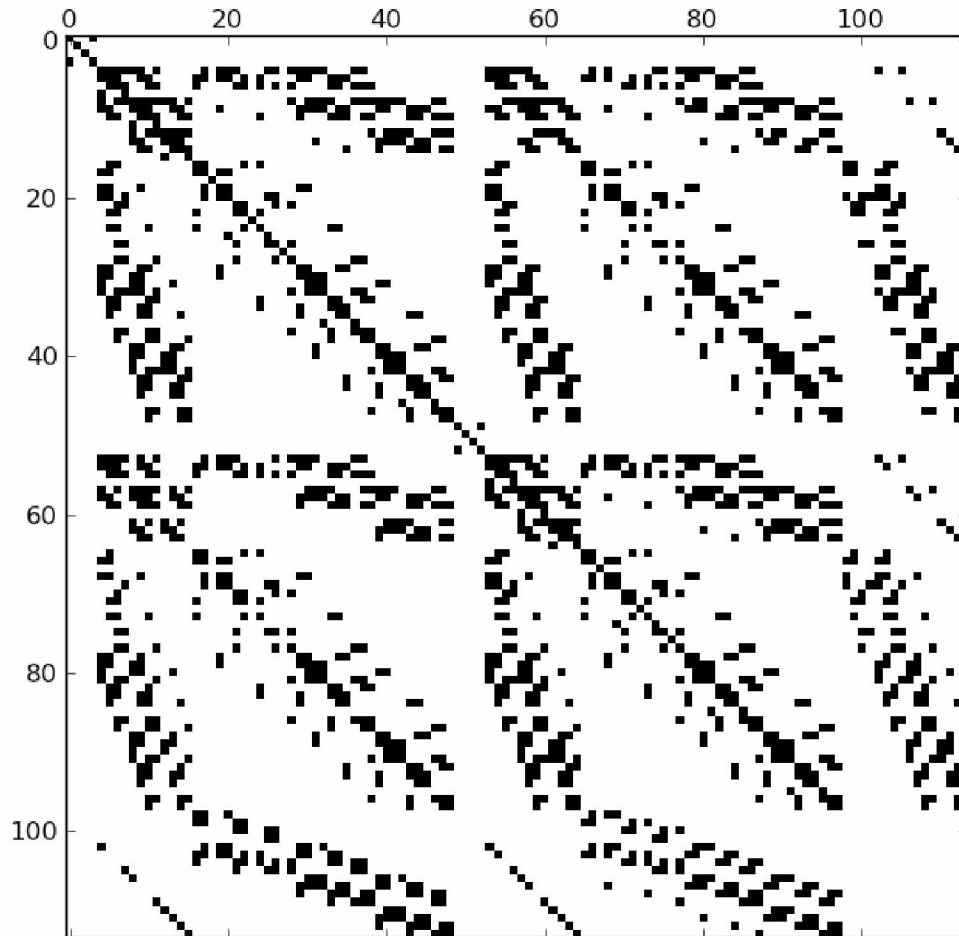


Figure 4.5. Sparsity structure with both Dirichlet and periodic conditions.

equation but the same number of unknowns, a situation that would lead to an underdetermined system if we did not also impose the constraint

$$\hat{u}_{i_1} - \hat{u}_{i_2} = 0 \quad (4.44)$$

which makes the velocity \mathbf{u} periodic. This gives a square system once again. We illustrate the sparsity structure of this modified system in Figure 4.5. Note that our naïve enforcement of the periodicity condition has destroyed the symmetry.

The matched pair of mesh points in the lower corners of the rectangle deserve attention

as a special case. Because two numbers are each equal to a if and only if their sum is $2a$ and they are equal, our procedure for applying the periodic condition can be applied harmlessly to the diagonal subsystem if the imposed velocity at the bed is itself periodic. It is of course reasonable to restrict to periodic \mathbf{w} if we want to find a periodic \mathbf{u} .

4.4 Solution of the Linear System

The solution of large sparse systems of linear equations like the one constructed in the last section is a vast subject in its own right. Many direct and iterative methods are available to users of FEniCS. For the 2-dimensional simulations carried out in the next chapter, the systems are small enough to permit solution by direct methods on my desktop computer. I chose the `spooles` routine [AG99]. The three-dimensional simulations reported in [LJG⁺12] required solving systems with more than two million equations many times. Because the systems are nonsymmetric and indefinite, the iterative GMRES method forms the core of their algorithm. The details of the preconditioning and the special tactics adopted to exploit the block structure are beyond our scope here.

Chapter 5

A Numerical Stokes Solver with Error Analysis

5.1 A FEniCS-based Glaciological Stokes Solver

The previous chapter described the finite element method for solving the Stokes system of partial differential equations with boundary conditions of Dirichlet, periodic, and no-stress types. It is now easy to implement this technique on a computer using a freely-available general purpose finite element software package called FEniCS. In Figure 5.1 we give a concise script implementing the technique described above. This script is based on `IceTools`, a 2008 FEniCS-based nonlinear Stokes solver described in [Jar08], although there is one important difference which we will discuss in Section 5.3. In this section we use this script as an example in order to briefly point out some of the features of FEniCS and its accompanying `dolfin` module for Python. More information about FEniCS and a comprehensive tutorial can be found in [LMW12].

Mesh generation is accomplished by the call to `Rectangle` in line 9. The last two arguments indicate that each dimension of the domain is to be divided into three equal segments. Each subrectangle is then divided into two triangles as in Figure 4.2. The resulting `mesh` object consists of a 16×2 array containing the coordinates of the 16 nodes, together with an 18×3 array of integers wherein each row lists three nodes forming a triangle of the mesh.

A variety of discrete function spaces are available. The argument ‘‘CG’’ in lines 10 and 11 specifies continuity, and the arguments 2 and 1 specify piecewise quadratic and linear functions respectively. Having chosen these velocity and pressure approximation spaces \mathbf{V} and \mathbf{Q} , it is easy to form their Cartesian product \mathbf{W} . Line 34 defines a function U in \mathbf{W} ; its expansion in the basis described in the last chapter is available through `U.vector()`.

To impose a Dirichlet condition we must specify a part of the boundary and supply a function defined on that boundary. This is the object of lines 14-17; note that in this demo we are imposing the basal velocity $u|_{\Gamma_D} = 3 + 1.7 \sin\left(\frac{2\pi x}{L}\right)$ in meters per year.

To define a periodic boundary condition we must mark one of the two boundary zones that are to be matched and give a function that maps points \mathbf{x} on the unmarked boundary to points \mathbf{y} on the marked boundary in a bijective fashion. Here we mark the left boundary and supply the map that subtracts the length `Le` from the first coordinate.

```

1 from dolfin import *
2 """Set domain parameters and physical constants"""
3 Le,He = 4e3, 5e2 #length, height (m)
4 alpha = 1*pi/180 #slope angle (radians)
5 rho,g = 917, 9.81 #density (kg m-3), gravity (m sec-2)
6 mu = 1e14 #viscosity (Pa sec)
7 G = Constant((sin(alpha)*g*rho,-cos(alpha)*g*rho)) #body force
8 """Define a mesh and some function spaces"""
9 mesh = Rectangle(0,0,Le,He,3,3)
10 V = VectorFunctionSpace(mesh, "CG", 2) #pw quadratic (velocity)
11 Q = FunctionSpace(mesh, "CG", 1) #pw linear (pressure)
12 W = V * Q #product space
13 """Define the Dirichlet condition at the base"""
14 def LowerBoundary(x, on_boundary):
15     return x[1] < DOLFIN_EPS and on_boundary
16 SlipRate = Expression(("(3+1.7*sin(2*pi/%s*x[0]))/31557686.4"%Le," 0.0"))
17 bcD = DirichletBC(W.sub(0), SlipRate, LowerBoundary)
18 """Define the periodic condition on the lateral sides"""
19 class PeriodicBoundary_x(SubDomain):
20     def inside(self, x, on_boundary):
21         return x[0] == 0 and on_boundary
22     def map(self, x, y):
23         y[0] = x[0] - Le
24         y[1] = x[1]
25 pbc_x = PeriodicBoundary_x()
26 bcP = PeriodicBC(W.sub(0), pbc_x)
27 """Define the variational problem: a(u,v) = L(v)"""
28 (v_i, q_i) = TestFunctions(W)
29 (u_i, p_i) = TrialFunctions(W)
30 a = (0.5*mu*inner(grad(v_i)+grad(v_i).T, grad(u_i)+grad(u_i).T)\
31      - div(v_i)*p_i + q_i*div(u_i))*dx
32 L = inner(v_i, G)*dx
33 """Matrix assembly and solution"""
34 U = Function(W)
35 solve(a=L,U,[bcD,bcP])
36 """Split the mixed solution to recover u and p"""
37 (u, p) = U.split()

```

Figure 5.1. A numerical Stokes solver in 37 lines using FEniCS.

The variational form of the problem is defined in lines 28-32. The power of this software is apparent when we compare the command

```
a = (0.5*mu*inner(grad(v_i)+grad(v_i).T, grad(u_i)+grad(u_i).T)\
      - div(v_i)*p_i + q_i*div(u_i) )*dx
```

to the quantity

$$\frac{1}{2}\mu \int_{\Omega} (\nabla \mathbf{u}^T + \nabla \mathbf{u}) : (\nabla \mathbf{v} + \nabla \mathbf{v}^T) - \int_{\Omega} p \nabla \cdot \mathbf{v} + \int_{\Omega} q \nabla \cdot \mathbf{u}$$

which formed the left hand side of the variational equation (4.22). The actual computation of these integrals for our particular mesh is done automatically.

The linear system of equations is assembled and solved by the `solve` command, which takes as arguments the variational formulation, a `Function` object to store the solution, and a list of boundary conditions. This command uses a default direct solver. If we want to specify a solver or examine the assembled matrix, we can take more control over this process by replacing the `solve` command with a sequence such as

```
A,bb = assemble_system(a,L,bcD)
bcP.apply(A,bb)
solve(A,U.vector(),bb,'spooles')
```

which replicates the assembly process described in the last chapter. The symmetric system of Figure 4.4 is obtained by calling `spy(A.array())` following the `assemble_system` command, using the module `pylab`. The periodic conditions are applied in an asymmetric manner in the next line, producing the system depicted in Figure 4.5. Finally the system is solved with the sparse LU solver `spooles` [AG99].

This script can easily be modified for the three-dimensional case. We replace `Rectangle` with `Box` in line 9, add a new periodic boundary condition, and make a few minor adjustments such as adding a third component to the gravity vector `G`.

5.2 Error Analysis

The analytical results of Chapter 3 allow us to measure the errors of our numerical solver directly. In this section we give numerical evidence that the FEM solutions converge to the analytical solutions and we quantify the convergence rate in several norms.

Recall that we are imposing a basal velocity consisting of a single sine frequency. In this case the formulas (3.54), (3.56), and (3.68) giving exact solutions reduce to the simpler expressions:

$$u(x, z) = \frac{\lambda_1 H^2 a_1 \sin(\lambda_1 x)}{\lambda_1^2 H^2 + \cosh^2(\lambda_1 H)} \left[\lambda_1 \cosh(\lambda_1 z) - \frac{1}{H} \cosh(\lambda_1 H) \left(\sinh(\lambda_1(z - H)) \right. \right. \quad (5.1)$$

$$\left. \left. + \lambda_1 z \cosh(\lambda_1(z - H)) \right) + \frac{\cosh(\lambda_1 H) - \lambda_1 H \sinh(\lambda_1 H)}{\lambda_1 H^2} \cdot \left(\cosh(\lambda_1(z - H)) \right. \right.$$

$$\left. \left. + \lambda_1 z \sinh(\lambda_1(z - H)) \right) \right] + a_0 + \frac{g_1 H}{\mu} z - \frac{g_1}{2\mu} z^2$$

$$w(x, z) = \frac{-\lambda_1^2 H^2 a_1 \cos(\lambda_1 x)}{\lambda_1^2 H^2 + \cosh^2(\lambda_1 H)} \left[\sinh(\lambda_1 z) - \frac{1}{H} \cosh(\lambda_1 H) z \sinh(\lambda_1(z - H)) \right. \quad (5.2)$$

$$\left. + \frac{\cosh(\lambda_1 H) - \lambda_1 H \sinh(\lambda_1 H)}{\lambda_1 H^2} z \cosh(\lambda_1(z - H)) \right]$$

$$p(x, z) = g_2(z - H) + \frac{2\mu\lambda_1^2 H a_1 \cos(\lambda_1 x)}{\lambda_1^2 H^2 + \cosh^2(\lambda_1 H)} \left[\sinh(\lambda_1 z) - \frac{\cosh(H\lambda_1)}{\lambda_1 H} \cosh(\lambda_1(z - H)) \right]. \quad (5.3)$$

We use the parameters appearing in the script of Figure 5.1, *i.e.* $L = 4000$, $H = 500$, $a_0 = 3/31557686.4$, $a_1 = 1.7/31557686.4$, $\lambda_1 = \pi/2000$, $\mu = 10^{14}$, $\mathbf{g} = 9.81 * 917(\sin(1), -\cos(1))$. Note that with $H = 500$, the frequently occurring quantity $\lambda_1 H$ is equal to $\pi/4$.

We write these exact formulas as **Expression** objects. For example, the pressure is represented by

```
p_E = "%s*(x[1] - %s)+ 2*%s*pi/4*%s*%s*cos(%s*x[0])/(pow(pi,2)/16*pow(\
  cosh(pi/4),2))*(sinh(%s*x[1]) - 4*cosh(pi/4)/pi*cosh(%s*x[1]-pi/4))"\
  %(g2,He,mu,La1,a1,La1,La1,La1)
p_E_Expr = Expression(p_E)
```

FEniCS provides automatic computations of errors in several norms, but only by comparing **Function** objects. To make use of this capacity we must first interpolate the exact solutions using the command `p_e = interpolate(p_E_Expr, Q1)` after defining the interpolation space **Q1**. This interpolation, however, introduces further errors which are difficult to separate from the original numerical errors.

We therefore use a direct comparison that avoids interpolation altogether. The FEM

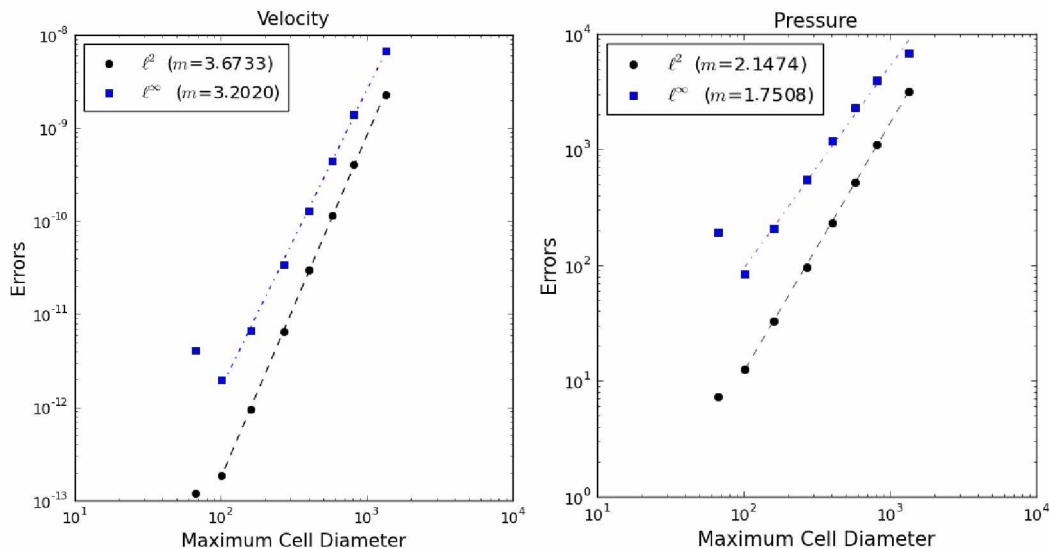


Figure 5.2. Errors in FEM velocity and pressure plotted against maximum element diameter, together with convergence rates m .

implementation gives solutions \mathbf{u} and \mathbf{p} stored as vectors expanding these functions in the basis described in the previous chapter. The entries are the function values at mesh points (or in the case of velocity, edge midpoints as well). We evaluate the exact solutions at these points as well and measure the difference between these vectors in the ℓ^2 and ℓ^∞ norms.

Errors for the the script given above are reported in Figure 5.2. We use an aspect ratio of 1:8 for the domain and our mesh construction divides the domain into an equal number of vertical and horizontal pieces. We let the number of subdivisions range from 3 (as it appears in line 9 in Figure 5.1) up to 60. For these meshes, the maximum element diameter ranges from 1344 down to 67. Experimentation shows that numerical errors start to interfere with convergence on meshes of maximum diameter less than 100. The convergence rates m are obtained by fitting a first-degree polynomial to the logs of the data appearing in Figure 5.2 (using the normal equations to solve the least-squares problem).

5.3 Improvement of Ictools, a FEM Stokes Solver

One consequence of distributing open-source software is the possibility that users will improve it by identifying errors. This section identifies an error in the variational form used

in Ictools and suggests a simple correction.

The paper [Jar08] does not give details about the variational formulation used to solve the linear problem. The demo uses the forms

$$\begin{aligned} \mathbf{a} &= (\text{inner}(\text{grad}(\mathbf{v}_i), \text{nu} * \text{grad}(\mathbf{u}_i)) - \text{div}(\mathbf{v}_i) * \mathbf{p}_i + \mathbf{q}_i * \text{div}(\mathbf{u}_i)) * \text{dx} \\ \mathbf{L} &= \text{inner}(\mathbf{v}_i, \mathbf{f}) * \text{dx} \end{aligned}$$

and so the original Ictools code evidently solves the variational equality

$$\mu \int_{\Omega} \nabla \mathbf{v} : \nabla \mathbf{u} - \int_{\Omega} p \nabla \cdot \mathbf{v} + \int_{\Omega} q \nabla \cdot \mathbf{u} = \int_{\Omega} \mathbf{g} \cdot \mathbf{v}. \quad (5.4)$$

This equation is more common in mathematics texts than (4.22). For example, it appears on p. 279 of [DH03] if we take $\mathbf{t} = \mathbf{0}$ in the Neumann condition

$$-p\mathbf{n} + \mu \frac{\partial \mathbf{u}}{\partial \mathbf{n}} = \mathbf{t} \quad (5.5)$$

applied at the upper surface. With $\mathbf{t} = \mathbf{0}$ and since $\mathbf{n} = (0, 1)$ on the upper surface, we can write (5.5) in the coordinate form

$$\mu \frac{\partial u}{\partial z} = 0 \quad (5.6)$$

$$-p + \mu \frac{\partial w}{\partial z} = 0. \quad (5.7)$$

It is unclear, however, why this Neumann condition is equivalent to the stress-free condition $\sigma \cdot \mathbf{n} = 0$. Indeed, we can use the analytical results from [BR85] as discussed in Chapter 3 to show that the two conditions are not equivalent. Recall that we gave an exact formula for $\frac{\partial u}{\partial z}|_{z=H}$ in (3.83). In the simple case where the imposed basal velocity has the form $3 + 1.7 \sin\left(\frac{2\pi L}{x}\right)$, this gives

$$\frac{\partial u}{\partial z}(x, H) = -\frac{\lambda_1^2 H \cosh(\lambda_1 H)}{\lambda_1^2 H^2 + \cosh^2(\lambda_1 H)} \cdot 1.7 \sin(\lambda_1 x) \quad (5.8)$$

with $\lambda_1 = 2\pi/L = 2\pi/4000$. Clearly this quantity does not vanish for all x , and so the analytical solution \mathbf{u} violates (5.6) and also (5.5). On the other hand, we showed in Section 3.8 that this velocity solution along with the corresponding pressure yields zero stress at the

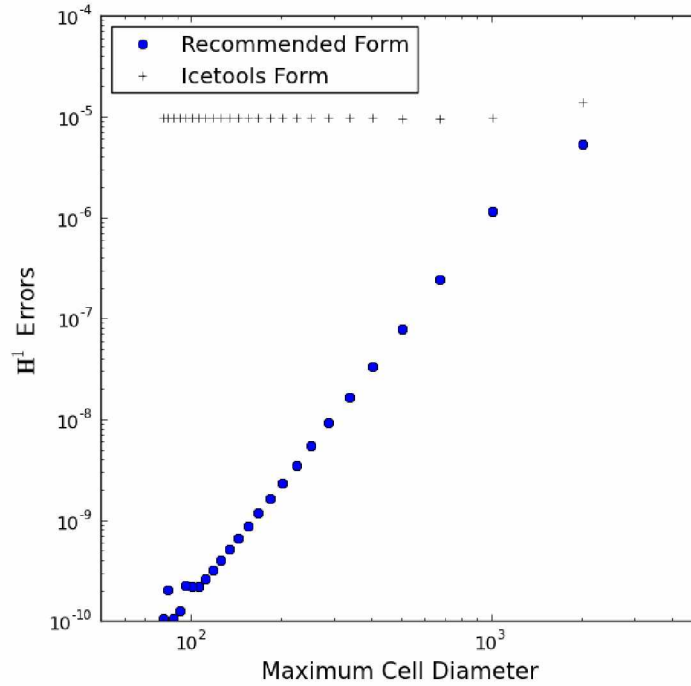


Figure 5.3. \mathbf{H}^1 convergence of velocity using the recommended form (4.22) and the Icetools form (5.4).

surface. In light of this counterexample, (5.4) and (5.5) should be regarded as unsuitable for use in a glaciological context.

To give numerical evidence, we try both variational forms for increasingly fine meshes and compare the results with exact solutions. The errors for the current Icetools code and for the recommended script illustrated above are plotted in the \mathbf{H}^1 norm in Figure 5.3. The errors were computed by the command `errornorm` following interpolation of the exact solution to the finite-dimensional velocity space. The variational form (5.4) does not generate convergence to the analytical solution.

There is one exception to this conclusion, and this exception is exactly the case that was used for verification in [Jar08]. If a no-slip condition applies everywhere on the lower boundary, (3.83) yields $\frac{\partial u}{\partial z}(x, H) = 0$ and (3.88) yields $\frac{\partial w}{\partial z}(x, H) = 0$. Therefore we can enforce (5.5) by taking $p = 0$ at the surface, and the stress-free condition is then equivalent to the Neumann condition (5.5). The nonlinear model proposed in [Jar08] is a Picard

iteration where the linear problem we have considered is solved repeatedly. That paper describes a verification where the output was tested numerically against a known exact solution for the nonlinear case with a no-slip condition at the base. The first linear problem in the iteration was precisely the special case where (4.22) and (5.4) give the same answer. It is plausible that the two bilinear forms are equivalent whenever the flow is parallel, which remains the case throughout this Picard iteration. The Icetools model was never tested against a non-parallel exact solution such as that given by [BR85] in the linear case. The presence of such an error in a recent published model demonstrates the continued relevance of exact solutions such as those in [BR85].

Fortunately for users of Icetools, the problem is very easy to remedy. The line

```
a = (inner(grad(v_i), nu*grad(u_i)) - div(v_i)*p_i + q_i*div(u_i))*dx
```

should be replaced by

```
a = (0.5*nu*inner(grad(v_i)+grad(v_i).T, grad(u_i)+grad(u_i).T)\
      - div(v_i)*p_i + q_i*div(u_i) )*dx
```

This suffices to give the superior results of Figure 5.3 for non-parallel linear-viscosity flows.

Chapter 6

Conclusion

In this work we considered the problem of determining linear Stokes flows on a rectangle with an arbitrary imposed basal velocity, a no-stress condition at the surface, and periodic conditions on the lateral sides. We extended an earlier result giving exact solutions by providing expressions for the pressure and basal stress. We then used the finite element method to solve the same problem and discussed the convergence of an implementation in FEniCS.

This work could be extended in several directions in the future. On the numerical side, we can address the nonlinear problem by iterating the algorithm presented in Chapter 5. Generating more interesting domains and extending the algorithm to 3D problems should both be straightforward in FEniCS. Following [LJG⁺12], we can implement the linear sliding law instead of the Dirichlet condition at the base. This would provide a simple open-source nonlinear Stokes solver, verified in the linear case against the exact solutions of Chapter 3. On the analytical side, replacing the Dirichlet condition with the linear sliding law for constant-viscosity flow may lead to another tractable problem and more exact solutions. We could then impose the friction profile $\beta^2(x)$ instead of obtaining it as an output.

Bibliography

- [Ach90] D. J. Acheson. *Elementary Fluid Dynamics*. Oxford University Press, New York, 1990.
- [AG99] Cleve Ashcraft and Roger Grimes. SPOOLES: an object-oriented sparse matrix library. In *Proceedings of the Ninth SIAM Conference on Parallel Processing for Scientific Computing 1999 (San Antonio, TX)*, page 10, Philadelphia, PA, 1999. SIAM.
- [Bat00] G. K. Batchelor. *An Introduction to Fluid Dynamics*. Cambridge University Press, Cambridge, UK, 2000.
- [BR85] M. J. Balise and C. F. Raymond. Transfer of basal sliding variations to the surface of a linearly viscous glacier. *Journal of Glaciology*, 31(109), 1985.
- [CP10] K. M. Cuffey and W. S. B. Paterson. *The Physics of Glaciers*. Academic Press, Amsterdam, Boston, 4th edition, 2010.
- [DH03] J. Donea and A. Huerta. *Finite Element Methods for Flow Problems*. Wiley, New York, 1st edition, 2003.
- [DM05] L. Debnath and P. Mikusinski. *Introduction to Hilbert Spaces with Applications, Third Edition*. Academic Press, 3rd edition, 2005.
- [Ern04] A. Ern. *Theory and Practice of Finite Elements*. Springer, Berlin, Heidelberg, 2004.
- [ESW05] H. C. Elman, D. J. Silvester, and A. J. Wathen. *Finite Elements And Fast Iterative Solvers - With Applications in Incompressible Fluid Dynamics*. Oxford University Press, New York, 2005.
- [GB09] R. Greve and H. Blatter. *Dynamics of Ice Sheets and Glaciers (Advances in Geophysical and Environmental Mechanics and Mathematics)*. Springer, 1st edition. edition, 8 2009.
- [Goo82] A. M. Goodbody. *Cartesian tensors - with applications to mechanics, fluid mechanics and elasticity*. E. Horwood, Chichester, 1982.

- [Jar08] A. H. Jarosch. Icetools: A full stokes finite element model for glaciers. *Computers & Geosciences*, 34:1005–1014, 2008.
- [Jóh92] Tómas Jóhannesson. *Landscape of Temperate Ice Caps*. PhD thesis, University of Washington, 1992.
- [LJG⁺12] W. Leng, L. Ju, M. Gunzberger, S. Price, and T. Ringler. A parallel high-order accurate finite element nonlinear stokes ice sheet model and benchmark experiments. *Journal of Geophysical Research*, 117, 2012.
- [LMW12] A. Logg, K. Mardal, and G. Wells, editors. *Automated Solution of Differential Equations by the Finite Element Method: The FEniCS Book (Lecture Notes in Computational Science and Engineering)*. Springer, Berlin, Heidelberg, 2 2012.
- [Pir89] O. Pironneau. *Finite element methods for fluids*. Wiley, New York, 1989.
- [QV94] A. Quarteroni and A. Valli. *Numerical Approximation of Partial Differential Equations*. Springer, Berlin, Heidelberg, 1st edition, 1994.
- [TS63] A. N. Tikhonov and A. A. Samarskii. *Equations of Mathematical Physics*. Pergamon Press, Oxford, 1963. Translated by A.R.M. Robson and P. Basu and edited by D. M. Brink.
- [Wor09] G. Worster. *Understanding Fluid Flow*. Cambridge University Press, Cambridge, 1st edition, 2009.